Available online at www.sciencedirect.com
SCIENCE DIRECT
Biochemical Pharmacology 69 (2005) 761–780
Biochemical Pharmacology
www.elsevier.com/locate/biochempharm

Regulation of lipid raft proteins by glimepiride- and insulin-induced glycosylphosphatidylinositol-specific phospholipase C in rat adipocytes

Günter Müller*, Andrea Schulz, Susanne Wied, Wendelin Frick

Sanofi-Aventis, TD Metabolism, Industrial Park Frankfurt-Höchst, Bldg. H821, 65926 Frankfurt am Main, Germany

Received 11 August 2004; accepted 25 November 2004

Abstract

The insulin receptor-independent insulin-mimetic signalling provoked by the antidiabetic sulfonylurea drug, glimepiride, is accompanied by the redistribution and concomitant activation of lipid raft-associated signalling components, such as the acylated tyrosine kinase, $pp59^{Lyn}$, and some glycosylphosphatidylinositol-anchored proteins (GPI-proteins). We now found that impairment of glimepiride-induced lipolytic cleavage of GPI-proteins in rat adipocytes by the novel inhibitor of glycosylphosphatidylinositol-specific phospholipase C (GPI-PLC), GPI-2350, caused almost complete blockade of (i) dissociation from caveolin-1 of $pp59^{Lyn}$ and GPI-proteins, (ii) their redistribution from high cholesterol- (hcDIGs) to low cholesterol-containing (lcDIGs) lipid rafts, (iii) tyrosine phosphorylation of $pp59^{Lyn}$ and insulin receptor substrate-1 protein (IRS-1) and (iv) stimulation of glucose transport as well as (v) inhibition of isoproterenol-induced lipolysis in response to glimepiride. In contrast, blockade of the moderate insulin activation of the GPI-PLC and of lipid raft protein redistribution by GPI-2350 slightly reduced insulin signalling and metabolic action, only. Importantly, in response to both insulin and glimepiride, lipolytically cleaved hydrophilic GPI-proteins remain associated with hcDIGs rather than redistribute to lcDIGs as do their uncleaved amphiphilic versions. In conclusion, GPI-PLC controls the localization within lipid rafts and thereby the activity of certain GPI-anchored and acylated signalling proteins. Its stimulation is required and may even be sufficient for insulin-mimetic cross-talking to IRS-1 in response to glimepiride *via* redistributed and activated $pp59^{Lyn}$.

Keywords: Insulin signalling; Sulfonylurea action; Lipid rafts; Glycosylphosphatidylinositol; Rat adipocytes

1. Introduction

Most mammalian cells and tissues express a number of GPI-proteins, the majority of them with their GPI anchor embedded in the outer leaflet of the PM [1], as well as some lipases, the (G)PI-PLC/D, which may control down-regulation of GPI-protein cell surface expression and simultaneously up-regulation of the soluble protein moiety released into circulation. In fact, soluble forms of GPI-proteins have been detected in human plasma, such as 5′-Nuc [2], Thy-1 [3], aP [4] and CD16 receptors [5], and GPI-PLC have been found in human neutrophils [5], bovine brain [6], rat intestine [7] and a human carcinoma cell line [8]. The GPI anchor consisting of three mannose residues and a non-acetylated glucosamine, one end of which amide-linked to the protein moiety *via* a phosphoethanolamine bridge and the other end glycosidically linked to the 6-hydroxyl group of PI, is cleaved by (G)PI-PLC/D releasing diacylglycerol or phosphatidic acid,

Abbreviations: AChE, acetylcholinesterase; aP, alkaline phosphatase; BSA, bovine serum albumin; CBD(P), caveolin-binding domain (peptide); cIP, *myo*-inositol-1,2-cyclic phosphate; CRD, cross-reacting determinant; CSD, caveolin-scaffolding domain; DMSO, dimethylsulfoxide; DTT, dithiothreitol; EDTA, ethylene diamine tetraacetic acid; Gce1, GPI-anchored cAMP-binding ectoprotein 1; Glut4, glucose transporter isoform 4; GPI, glycosylphosphatidyl-inositol; GPI-PLC/D, GPI-specific phospholipase C/D; GPI-protein, GPI-anchored plasma membrane protein; HSL, hormone-sensitive lipase; IR(β), insulin receptor (β-subunit); IRS-1/2, insulin receptor substrate-1/2; lc/hcDIGs, low/high cholesterol-containing detergent-insoluble glycolipid-enriched membrane microdomains (lipid rafts); LPL, lipoprotein lipase; m-β-CD, methyl-β-cyclodextrin; MES, morpholinoethane sulfonic acid; NBD-FA, 12-((7-nitrobenz-2-oxa-1,3-diazol-4-yl)amino)dodecanoic acid; NEM, *N*-ethylmaleimide; 5′-Nuc, 5′-nucleotidase; p115, 115 kDa PIG receptor protein; PC, phosphatidylcholine; PI, phosphatidylinositol; PIG, phosphoinositolglycans; PI3K, phosphatidylinositol-3′-kinase; PI/PC-PL, PI/PC-specific phospholipase; PL, pancreatic lipase; PLA_2/C/D, phospholipase A2/C/D; PM, plasma membranes; SDS-PAGE, sodium dodecylsulfate polyacrylamide gel electrophoresis; TLC, thin layer chromatography; TX-100/114, Triton X-100/114

* Corresponding author. Tel.: +49 69 305 4271; fax: +49 69 305 81901.
E-mail address: guenter.Mueller@sanofi-aventis.com (G. Müller).

0006-2952/$ – see front matter © 2004 Elsevier Inc. All rights reserved.
doi:10.1016/j.bcp.2004.11.014

respectively, and leaving a terminal inositolglycan structure at the protein moiety harbouring (PIG) or lacking a (cyclic) phosphate residue [9].

Endogenous GPI-PLC activity has been described for porcine proximal tubules [10] and rat liver membranes [11], but the protein and the gene of a mammalian GPI-PLC have not been elucidated so far. The situation is different for the mammalian GPI-PLD from serum, which acts on its substrate after its uptake from the serum in the lysosomal compartment [12] and degrades the GPI anchor of GPI-proteins following their endocytosis and trafficking to lysosomes [13]. Some GPI-proteins, such as 5′-Nuc and aP in yeast and rodent adipocytes, do not seem to be released as soluble versions from the cell surface upon lipolytic cleavage of their GPI anchors by a GPI-PLC in vitro and in vivo [14–16]. Additional mild salt and/or limited trypsin cleavage is required for recovery of the protein moieties of some lipolytically cleaved GPI-proteins from the soluble fraction/medium indicative for the existence of a receptor protein [17]. In these cases, GPI-PLC action apparently does not affect the localization, topology or half-life time of GPI-proteins but rather may modify their function in the course of their conversion from the amphiphilic into the hydrophilic version [18]. The often observed negative effect of GPI modification on the catalytic or binding activity of the enzyme/protein moiety attached [19–24] may result from conformational restraints on the active site which undergo relaxation upon GPI anchor cleavage.

In eukaryotes, some GPI-PLC/D are up-regulated by nutritional signals, such as glucose in yeast [15,16,25], where lipolytic processing of GPI-proteins seems to play a role during biogenesis of the cell wall [26], and by glucose as well as certain hormones, growth factors and drugs (e.g. insulin, glimepiride) in rodent adipocytes, myocytes and human endothelial cells [27–31]. In particular, the antidiabetic drug glimepiride, which lowers blood glucose predominantly by stimulation of insulin release from pancreatic β-cells and, in addition, to a minor degree by mimicking metabolic insulin action in peripheral tissues, such as activation of glucose transport in muscle cells and inhibition of lipolysis in adipocytes [32,33], has been demonstrated to activate a GPI-PLC. Upon treatment of primary or cultured rodent adipocytes with pharmacological concentrations of this sulfonylurea, a potent amphiphilic-to-hydrophilic conversion of a subset of GPI-proteins, such as 5′-Nuc, aP and Gce1, by activation of a GPI-PLC has been observed [14,17,30]. The functional and physiological significance of the insulin- and glimepiride-regulated lipolytic cleavage of GPI-proteins in mammalian cells is not well understood at present. Its study is hampered by unavailability of the gene structure and of specific inhibitors for the mammalian cell-associated GPI-PLC so far.

Here we characterize a synthetic inositol derivative, GPI-2350, which inhibits the well-characterized bacterial, trypanosomal and serum (G)PI-PLC/D with high potency and selectivity. Using GPI-2350, which almost completely down-regulates the insulin- and glimepiride-inducible GPI-PLC in intact rat adipocytes, a major role for this enzyme in metabolic insulin signalling and action in these cells could be excluded. In contrast, activation of the GPI-PLC turned out to be indispensable for the insulin-mimetic effects of glimepiride *via* the recently described IR-independent cross-talk from DIGs to the IRS-1 protein [32,34]. DIGs, which are detergent-insoluble glycolipid-enriched membrane microdomains or so-called lipid rafts, are expressed in high number in the PM of many terminally differentiated cells, such as adipocytes, and specifically serve as platforms for membrane-mediated biological processes, including signal transduction and trafficking and sorting of proteins and lipids [35–37]. They are enriched in cholesterol and (glyco)sphingolipids in the exoplasmic leaflet and in phospholipids with saturated acyl chains and cholesterol in the cytoplasmic leaflet forming a liquid-ordered phase within the bilayer. DIGs are characterized by insolubility in 1% TX-100 at 4 °C for 1 h and low buoyant density upon sucrose gradient centrifugation. Based on these criteria, certain GPI-anchored, acylated and transmembrane signalling proteins have been found to be enriched in DIGs versus non-DIG areas of the PM. Furthermore, DIGs are not homogenous in composition and structure since subspecies of higher (hcDIGs) and lower cholesterol (lcDIGs) content can be distinguished from one another on the basis of their lower and higher buoyant density, respectively [38]. Strikingly, the stimulus-induced redistribution of certain GPI-anchored as well as acylated signalling proteins from hcDIGs to lcDIGs was blocked by GPI-2350. This finding hints to a role of the mammalian GPI-PLC in the control of the localization and activation of signalling proteins within DIGs during signal transduction across the PM of adipocytes.

2. Materials and methods

2.1. Agents

Human recombinant insulin, PIG-41 (structure and synthesis see Ref. [39]) and glimepiride (trade name Amaryl) were supplied by the medicinal chemistry and synthesis departments of Aventis Pharma Germany. NBD-FA was synthesized as described previously [40]. Collagenase (Worthington, CLS, type I, 250 units/mg) was provided by Biochrom. LPL (affinity-purified) from bovine milk, PLA_2 (honey bee venom), crude porcine PL, recombinant PC/PI-PLC (*Bacillus cereus*), crude PLD (cabbage) and defatted BSA (fraction V) were delivered by Sigma/Aldrich. Crude PI-PLC (rat liver) and proteinase inhibitors were purchased from Roche Molecular Biochemicals. Recombinant GPI-PLC (*Trypanosoma brucei*) and anti-

CRD antibodies were obtained from Oxford Glycosystems. Inhibitors of PLA_2 ($AACOCF_3$) and PLC (U 73122) were supplied by Tocris. Bisbodipy-C_{11}-PC was bought from Molecular Probes. Lipids were purchased from Avantis Polar Lipids. Antibodies for immunoprecipitation of caveolin-1 (clone C060) and immunoblotting of caveolin-1 (rabbit) and $pp59^{Lyn}$ (clone 32) were obtained from Transduction Laboratories. Antibodies for immunoblotting of phosphotyrosine (clone 4G10) were made available by Upstate Biotechnology. Antibodies (rabbits, affinity-purified) for immunoblotting of IRS-1 (against total human recombinant protein expressed in insect cells), 5′-Nuc (rat) and aP (bovine) were prepared by Biotrend. ECL Renaissance chemiluminescence detection kit was obtained from NEN/DuPont. TX-100 was delivered by Merck. Lubrol-WX (Lubrol 17A17) was purchased from Serva. Sprague-Dawley rats were provided by Charles-River Laboratories and handled in agreement with paragraph 6 of the German Animal Protection Law. All other materials were obtained as described previously [38–43].

2.2. Synthesis of GPI-2350

As starting material, racemic 1,4,5,6-tetra-*O*-benzyl-*myo*-inositol **1** was prepared by a published procedure [44]. Compound **1** was then phosphorylated with dodecylphosphonic dichloride in the presence of triethylamine and dimethyl-aminopyridine to yield tetra-*O*-benzyl-*myo*-inositol-1,2-cyclo-dodecylphosphonic acid **2**. By catalytic hydrogenation with 10% Pd on charcoal compound **2** was debenzylated to *myo*-inositol-1,2-cyclo-dodecyl-phosphonic acid **3** (GPI-2350) as a mixture of diastereomeres. For synthesis of product **2** (Fig. 1), 1 g (1.8 mmol) of product **1** was dissolved in 60 ml of methylene chloride and 1 ml of triethylamine, 200 mg dimethyl-aminopyridine and 1 g (10 mmol) of dodecylphosphonic dichloride were added. This reaction solution was allowed to stand (45 min, 25 °C). Then 50 ml of ethyl acetate were added and the mixture was filtered on silical gel. After concentration of the solvent, the residue was purified by flash chromatography (*n*-heptane/ethyl acetate, 1/1, by vol.). Yield of product **2**: 580 mg (43%) of a white amorphous solid. TLC: *n*-heptane/ethyl acetate (1/1, by vol.), $R_f = 0.7$. MS: $(M + Li)^+ = 761.4$, calculated $C_{60}H_{59}O_7P$, M = 754.9. For synthesis of product **3** (Fig. 1), 505 mg (0.67 mmol) of product **2** was dissolved in a mixture of 5 ml of ethyl acetate and 15 ml of methanol. After adding 700 mg of Pd (10%) on charcoal, the reaction mixture was hydrogenated (6 h, 1 atm H_2). Pd was filtered over silical gel and washed with 100 ml methanol. After concentration of the solvent, the residue was purified by flash chromatography (methylene chloride/methanol, 5/1, by vol.). Yield of product **3**: 179 mg (68%) of a white amorphous solid. TLC: methylene chloride/methanol (5/1, by vol.), $R_f = 0.15$. MS: $(M + Li)^+ = 401.2$, calculated $C_{18}H_{35}O_7P$, M = 394.4. Compound **3** is less stable in acidic than basic solvents. It is stable in methanol for days and as dried amorphous solid for years at 4 °C.

2.3. Preparation and incubation of rat adipocytes

Adipocytes isolated by digestion from epididymal fat pads of male rats (120–140 g, fed ad libitum, see Ref. [38]) were washed twice in KRH-buffer (20 mM Hepes/KOH, pH 7.4, 1.2 mM KH_2PO_4, 140 mM NaCl, 4.7 mM KCl, 2.5 mM $CaCl_2$, 1.2 mM $MgSO_4$) containing 1% (w/v) BSA and then incubated in the same medium supplemented with 100 μg/ml gentamycin, 100 nM 1-methyl-2-phenylethyladenosine, 0.5 U/ml adenosine deaminase, 1 mM sodium pyruvate and 5 mM D-glucose in the absence or presence of GPI-2350 (prepared as 10 mM stock solution in DMSO, the final DMSO concentration in the in vitro and adipocyte incubations was kept constant at 0.5% at any inhibitor concentration), insulin or glimepiride (prepared as described previously [14]) at 37 °C in a shaking water bath at constant bubbling with 5% CO_2/95% O_2 at a final titer of 100 μl of packed cell volume per ml incubation volume (determined by aspiration of small aliquots into capillary hematocrit tubes and centrifugation for 60 s in a microhematocrit centrifuge in order to determine the fractional occupation of the suspension by the adipocytes; 10% cytocrit corresponds to about 1.5×10^6 cells/ml) for the periods indicated.

2.4. Preparation of plasma membranes (PM) and lc/hcDIGs

Pre-treated and subsequently washed adipocytes were homogenized in lysis buffer (25 mM MES, pH 6.0, 140 mM NaCl, 2 mM EDTA, 0.5 mM EGTA, 0.25 M sucrose, 50 mM NaF, 5 mM sodium pyrophosphate, 10 mM glycerol-3-phosphate, 1 mM sodium orthovanadate and protease inhibitors) using a motor-driven Teflon-in-glass homogenizer (10 strokes). PM were obtained by differential centrifugation of the defatted post-nuclear infranatant (= cytosolic fraction) and then purified by two sequential centrifugation steps through sucrose and Percoll cushions as described previously [38,40] and finally suspended in 25 mM Tris/HCl (pH 7.4), 0.25 M sucrose, 1 mM EDTA at 2 mg protein/ml. hc/lcDIGs were obtained by the detergent method and discontinuous sucrose gradient centrifugation as reported previously [38]. The light-scattering opalescent bands at the 0.5–0.65 M (fractions 3 + 4) and 0.8–0.9 M (fractions 5 + 6) sucrose interfaces were collected as hcDIGs and lcDIGs, respectively, with density measurement using the refractive index. hc/lcDIGs were collected by centrifugation ($50{,}000 \times g$, 30 min, 4 °C) after three-fold dilution of the pooled gradient fractions with 25 mM MES (pH 6.5), 1% TX-100, 150 mM NaCl, and then characterized (immunoblotting, enzyme assays) by enrichment/deprivation of relevant marker proteins as described previously

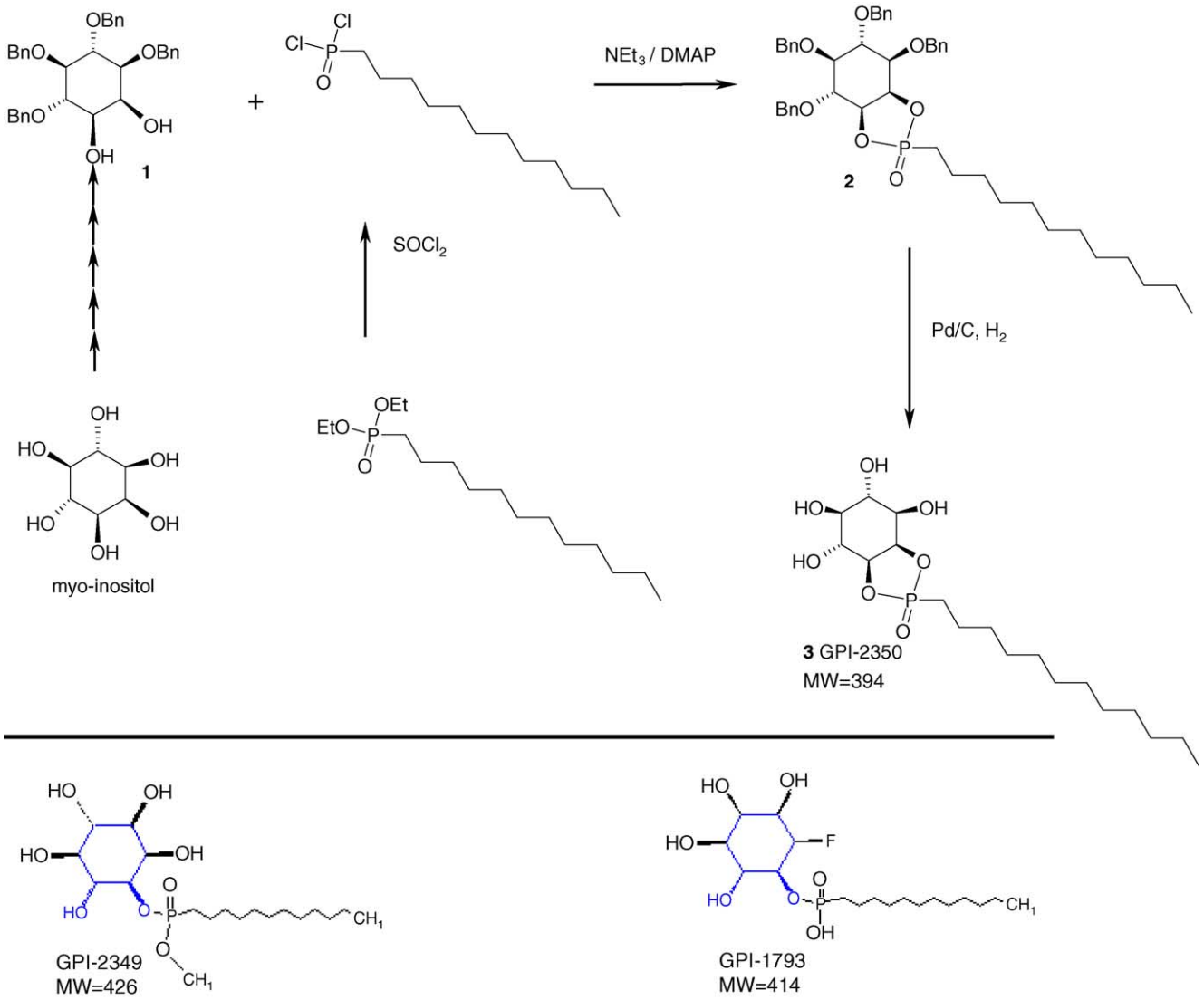

Fig. 1. Structure and synthesis of (G)PI-PLC inhibitors, GPI-2350, GPI-2349 and GPI-1793 (see Section 2).

[38,40] or subjected to TX-114 partitioning (see below). For immunoprecipitation of caveolin, DIGs were solubilized (1 h, 4 °C) in 10 mM Tris/HCl (pH 7.4), 150 mM NaCl, 1% TX-100, 60 mM β-octylglucoside, 0.3% deoxycholate, 5 mM EDTA, 0.5 mM EGTA, 1 mM sodium orthovanadate, 50 mM NaF, 1 μM microcystin and protease inhibitors and centrifuged (50,000 × *g*, 30 min). For direct immunoblotting, DIGs were solubilized in two-fold Laemmli sample buffer and centrifuged (10,000 × *g*, 5 min). The supernatants were used.

2.5. (G)PI-PLC/D assays

GPI-PLD (rat serum) was assayed according to published procedures [12,13] by incubation with 10 μl of human placental aP solution (100 U/ml in 10 mM Hepes/NaOH, pH 7.0, 150 mM NaCl) in 100 μl of 200 mM Tris/maleate (pH 7.0) and 1% Nonidet P-40 for 10 min at 37 °C and subsequent termination of the reaction by addition of 0.4 ml of ice-cold stop buffer (10 mM Hepes/NaOH, pH 7.0, 150 mM NaCl, 0.1 mM $MgCl_2$ and 0.01 mM zinc acetate). GPI-PLC (*T. brucei*) was assayed as described previously [45] by incubation with 5 μl of human placental aP solution (see above) in 50 μl of 50 mM Tris/HCl (pH 8.0), 0.25% Nonidet P-40 and 5 mM EDTA for 30 min at 37 °C and subsequent termination of the reaction by addition of 0.45 ml of stop buffer. PI-PLC (*B. cereus*) and adipocyte GPI-PLC (5–25 μg PM or hc/lcDIGs) were assayed according to a protocol adapted from Ref. [46] by incubation with 10 μl of bovine erythrocyte AChE solution (12 U/ml in 10 mM Tris/HCl, pH 7.4, 144 mM NaCl, 0.1% TX-100) in 100 μl of 20 mM Hepes/KOH (pH 7.8), 144 mM NaCl, 0.1% TX-100, 0.2 mM $MgCl_2$ for 1 h at 25 °C and subsequent termination by adding 5 μl of glacial acetic acid and then 0.4 ml of 10 mM Tris/HCl (pH 7.4), 144 mM NaCl. Each reaction

mixture was subjected to TX-114 partitioning (see below). The GPI-PLC/D activity was calculated as the amphiphilic-to-hydrophilic conversion of the GPI-protein substrates from the ratio of the activities of hydrophilic 5′-Nuc or AChE measured in the TX-114-depleted phase and the total activity measured before partitioning and corrected for the non-enzymatic background in the TX-114-depleted phase (accounting for 10–20% of the total activity) as revealed by blank incubations lacking (G)PI-PLC/D.

2.6. Other lipase assays

HSL and LPL were measured using a radiolabelled triolein droplet emulsion as described previously [47]. PL was determined by incubation of 0.25 mmol tributyrin in 2 ml of 5 mM Tris/HCl (pH 6.5), 6 mM sodium taurodeoxycholate, 150 mM NaCl, 1 mM $CaCl_2$ with porcine PL and colipase in the same buffer using a recording pH stat (stirring at 1000 rpm at 25 °C) with the pH adjusted to 6.5. PC-PLC was assayed by incubation of 0.2 ml of 10 mM dipalmitoyllecithin, 0.1 ml of 10 mM SDC and 0.1 ml of 0.03 M $CaCl_2$ with bacterial PC-PLC (in 50 mM Tris/HCl, pH 7.5, 0.1% BSA) for 10 min at 37 °C. The reaction was terminated by addition of 0.1 ml of 50% TCA and subsequently of 2.5 ml of chloroform/methanol (66/33/1, by vol.). After centrifugation (1500 × *g*, 15 min), 0.2 ml portions of the upper methanol/water phase (∼1.33 ml) was removed, supplemented with 0.5 ml of 60% $HClO_4$, then heated at 170 °C for 1 h and finally analyzed for inorganic phosphate. Mammalian PI-PLC was measured by incubation of 0.1 ml of 10 mM PI, 0.1 ml of 0.8% sodium deoxycholate, 0.1% BSA, 0.2 ml of 100 mM sodium borate (pH 7.5) and rat liver PI-PLC for 20 min at 37 °C. The reaction was terminated and further processed as described for the PC-PLC. PLD (cabbage) was assayed with 1.6 mM [U-^{14}C]PC (∼2000–4000 dpm/nmol) in 250 μl of 40 mM Hepes/KOH (pH 6.0), 4 mM $CaCl_2$. After incubation for 30 min at 37 °C, the reaction was terminated by addition of 5 ml of chloroform/methanol (2/1, by vol.) containing carrier phosphatidic acid. After removal of water-soluble material, lipids contained in the final washed lower chloroform phase were transferred to a heat-activated silica gel plate and separated two-dimensionally using chloroform/methanol/ammonia (65/35/4, by vol.) in the first and chloroform/acetone/methanol/acetic acid/water (50720/10/10/5, by vol.) in the second dimension. Radioactive phosphatidic acid was detected by phosphorimaging. PLA_2 was determined according to a published procedure [48] with a unilamellar liposomal substrate consisting of 1-palmitoyl-2-palmitoyl-*sn*-glycerol-3-phosphocholine/bisbodipy-C_{11}-PC/phosphatidylglycerol/cholesterol (10/0.05/2/3, by vol.). Concentration–response curves were fitted using a Marquardt–Levenberg non-linear least squares algorithm. When plotted on log-linear axes, this equation results in hyperbolic curves (SigmaPlot software, Jandel Scientific).

2.7. Immunoprecipitation of caveolin

Solubilized DIGs (see above, 5–20 μg protein) were precleared by incubation with protein A/G-Sepharose and subsequent centrifugation (10,000 × *g*, 5 min). The supernatant was incubated (1 h, 4 °C) with anti-caveolin-1 antibodies (1:1000) preadsorbed on protein A/G-Sepharose (as described previously [42,45]) in 1 ml of 10 mM Tris/HCl (pH 7.4), 150 mM NaCl, 1% TX-100. The immune complexes were washed twice with the same buffer and then twice with buffer lacking TX-100 and finally subjected to SDS-PAGE performed in the absence of β-mercaptoethanol. The recovery of immunoprecipitated caveolin was normalized by homologous immunoblotting with anti-caveolin antibodies of the same blot following stripping of the membrane.

2.8. Immunoblotting

Polypeptides separated by SDS-PAGE were transferred to polyvinylidene difluoride membranes using the semidry procedure as described previously [42,49]. Washed membranes were incubated with anti-caveolin-1 (1:2000), anti-pp59^{Lyn} (1:1250), anti-aP (1:500), anti-5′-Nuc (1:750) and anti-IRS-1 (1:2000) antibodies for 4 h at 15 °C. Washed membranes were incubated with horseradish peroxidase-coupled secondary goat anti-mouse (1:2000) or goat anti-rabbit IgG (1:4000) antibodies. Labelled proteins were visualized by enhanced chemiluminescence.

2.9. TX-114 partitioning

Pelleted hc/lcDIGs (10–50 μg protein) or (G)PI-PLC reaction mixtures (0.5 ml) were separated into amphiphilic and hydrophilic proteins using partitioning between TX-114-enriched and depleted phases according to Bordier [50] by suspending in 1 ml or mixing with 0.5 ml, respectively, of ice-cold 25 mM Tris/HCl (pH 7.4), 144 mM NaCl containing 1 or 2% TX-114. After incubation for 1 h on ice, the mixture was layered onto a cushion of 0.4 ml of 0.25 M sucrose and 25 mM Tris/HCl (pH 7.4) on ice. Phase separation was induced by warming up to 37 °C and subsequent centrifugation (10,000 × *g*, 1 min). After re-extraction of the lower TX-114-enriched phase, aliquots of the pooled upper TX-114-depleted phase were measured for 5′-Nuc, aP and AChE activity or precipitated (15% polyethylene glycol 4000) for SDS-PAGE analysis.

2.10. Glucose transport assay

Glucose transport was determined as described previously [14] by incubation of 1–2 × 10^4 washed adipocytes with 2-deoxy-D-[2,6-^{3}H]glucose (50 μM final conc.; 0.33 μCi/ml) in 50 μl portions for 20 min at 37 °C in the absence or presence of 20 μM cytochalasin B. Unspecific uptake, diffusion and intercellular entrapment of glucose

(presence of cytochalasin B), which were subtracted from total cell-associated glucose (absence of cytochalasin B) in each case, accounted for up to 20% of the specific glucose transport.

2.11. Cholesterol determination

For determination of the cholesterol content, 50 μl portions of the gradient fractions were subjected to chloroform/methanol extraction. The chloroform phase was subjected to TLC analysis (silica gel 60, Merck, hexane/ethyl acetate 2/1). Dried plates were sprayed with 20% sulphuric acid and heated to 135 °C for 30 min. Under these conditions, cholesterol stains dark red while phospholipids result in a greenish colour. Plates were scanned in black/white reflection mode followed by quantification of the digital images using ImageQuant software. Linearity of the method was checked by analysing different amounts of the same sample.

2.12. Miscellaneous procedures

Electroporation was performed as described previously [41]. Lipolysis was determined as release of glycerol or fluorescent NBD-FA from prelabelled and isoproterenol-stimulated adipocytes according to published procedures [51]. Adipocyte Gce1 was detected by photolabelling of solubilized PM or hc/lcDIGs (10–50 μg protein) with 8-N_3-[^{32}P]cAMP and subsequent phosphorimaging as described previously [17]. Yeast Gce1 was prepared by metabolic labelling with *myo*-[U-^{14}C]inositol of *S. cerevisiae* cells and subsequent partial purification from isolated hcDIGs according to published procedures [14,18,25]. 5′-Nuc, aP and AChE activities were measured according to published procedures [7,52–54]. Protein was determined using the BCA protein determination kit from Pierce and BSA as calibration standard. SDS-PAGE was performed using precast gels (Novex, 10% Bis–Tris resolving gel, morpholinopropanesulfonic acid-SDS running buffer). Lumiimages were evaluated on a LumiImager using LumiImager software (Roche Diagnostics). Phosphor- and fluorescence images were processed and quantified using the Storm 860 PhosphorImager system (Molecular Dynamics). Figures were constructed using the Adobe Photoshop software (Adobe).

3. Results

3.1. Inhibition of (G)PI-PLC/D of various origin by compound GPI-2350 with high potency and selectivity

Current experimental data indicate that the catalytic mechanisms of cleavage of PI and (less efficiently) GPI by bacterial PI-PLC as well as of GPI and (less efficiently) PI by trypanosomal GPI-PLC are all similar. However, it was questionable whether this may also be true for the adipocyte GPI-PLC, considering the failure of mammalian PI-PLC generating the second messenger, inositol-trisphosphate, to accept GPI anchors and of bacterial PI-PLC to cleave phosphorylated PI [24].

Catalysis by bacterial and trypanosomal (G)PI-PLC requires a free OH-group at the inositol-2 position [55] compatible with a two-step mechanism for (G)PI-PLC action with PI first being cleaved to produce a cIP structure which is then hydrolyzed to inositol-1-phosphate [24]. The requirement for transient or stable cIP formation is consistent with the finding that GPI anchors with their inositol residue palmitoylated at the 1- or 2-position, such as that of human erythrocyte AChE, resist lipolytic cleavage [56]. The most potent inhibitors of trypanosomal GPI-PLC reported so far have both a fluoro group at the 2-position and a dodecyl-phosphonate at the 1-position of 2-deoxy-inositol [57]. Interestingly, differential inhibition of (G)PI-PLC from *B. cereus* and *T. brucei* by some of these compounds argues that the two enzymes belong to distinct mechanistic subclasses. Unfortunately, analogous data are not yet available for mammalian GPI-PLC. Assuming similarity in the substrate recognition and catalytic mechanisms between bacterial, trypanosomal and adipocyte (G)PI-PLC, we synthesized *myo*-inositol-1,2-cyclododecylphosphonic acid (GPI-2350) and two derivatives as putative inhibitors for the adipocyte enzyme (Fig. 1).

The effect of GPI-2350 on (purified or crude) *B. cereus* PI-PLC, *T. brucei* GPI-PLC and rat serum GPI-PLD was monitored by incubation with partially purified solubilized GPI-proteins under appropriate conditions (low or high detergent concentration) in the presence of increasing inhibitor concentrations (Fig. 2). GPI-2350 inhibited bacterial, trypanosomal and serum (G)PI-PLC/D with apparent IC_{50} of 10, 2 and 1 μM, respectively. GPI-2350 also blocked the rat adipocyte GPI-PLC with IC_{50} of 0.2–0.5 μM using as enzyme source solubilized PM, lcDIGs or hcDIGs and as substrate, AChE. To exclude putative unspecific detergent-like effects, which could be caused by the aryl phosphonic acid constituent of GPI-2350, in particular, if released upon incubation with total PM, the effect of dodecylphosphate was studied. At 20 μM it reduced cleavage of AChE by rat adipocyte GPI-PLC by up to 15%, irrespective of the enzyme source used (data not shown). This underscores the critical importance of the inositol moiety of GPI-2350 for efficient inhibition of the adipocyte GPI-PLC. To demonstrate its cleavage specificity, we used the GPI-protein, Gce1, prepared from *Saccharomyces cerevisiae* cells which had been metabolically labelled with *myo*-[^{14}C]-inositol. Incubation with hcDIGs, lcDIGs and solubilized PM generated in concentration- and time-dependent fashion a hydrophilic and ^{14}C-labelled version of Gce1, which was immunoprecipitated with anti-CRD antibodies raised against cIP (data not shown). As shown previously [15,25], these antibodies specifically recognize during immunoprecipitation

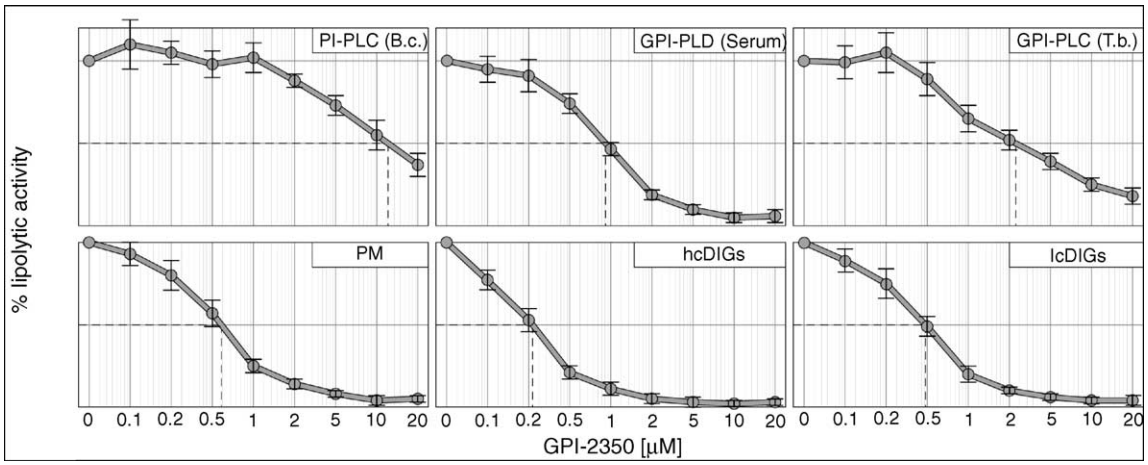

Fig. 2. Potency of GPI-2350. Purified (G)PI-PLC/D from *Bacillus cereus* (B.c.), rat serum and *Trypanosoma brucei* (T.b.) as well as total PM and hc/lcDIGs prepared from isolated rat adipocytes were incubated (10 min, 30 °C) with increasing concentrations of GPI-2350 and then assayed for amphiphilic-to-hydrophilic conversion of AChE by TX-114 partitioning (see Section 2). The lipolytic activity was calculated as % of the control reaction in the absence of GPI-2350 (set at 100%) hatched line, 50% lipolytic cleavage. Means ± S.D. of at least four independent incubations with AChE activity measurements in triplicate, each, are given.

and immunoblotting the GPI-PLC-cleaved versions of yeast and mammalian GPI-proteins harbouring the cIP epitope or with considerably lower efficacy the open inositol-monophosphate moiety. However, they fail to react with GPI-proteins to any significant extent upon cleavage with serum GPI-PLD or bacterial PI-PLC followed by enzymatic or chemical dephosphorylation or addition of excess of exogenous cIP (but not inositol). Thus, cross-reactivity of GPI-proteins with anti-CRD antibodies is strongly indicative for the hydrophilic versions of GPI-proteins lipolytically cleaved by (G)PI-PLC.

For elucidation of the type of inhibition of the adipocyte GPI-PLC by GPI-2350, intact hcDIGs were incubated with increasing concentrations of partially purified bovine AChE or yeast Gce1 in the presence of different inhibitor concentrations at low concentrations of TX-100 compatible with functional/structural integrity of the hcDIGs. The initial velocity of the lipolytic cleavages of the GPI-proteins was calculated from the amount of hydrophilic versions recovered with the detergent-depleted phase upon TX-114 partitioning. Direct and Lineweaver–Burk plots of the cleavage velocities versus the relative substrate concentrations of both AChE and Gce1 revealed a non-competitive/mixed type of inhibition of the hcDIGs-associated GPI-PLC by GPI-2350 (Fig. 3A–D). This argues for its interference with both the binding step of GPI-proteins to the hcDIGs–GPI-PLC interface and the catalytic step occurring within this interface. The K_i of 0.6 μM for GPI-2350 calculated on the basis of both GPI-proteins (Fig. 3E) was very similar to the apparent IC_{50} values (Table 1) in agreement with the competitive component of GPI-PLC inhibition by this inhibitor.

Next, the selectivity of GPI-2350 was studied. Several neutral lipases (HSL, PL, LPL) and PC/PI-specific phospholipases of different specificity (A_2, C, D) from various sources as well as bovine AChE, which were all known to operate *via* the so-called catalytic triad [58], were not significantly affected under conditions (50 μM) which blocked the bacterial, trypanosomal, serum and rat adipocyte (G)PI-PLC/D by 60–95% (Fig. 4). Two derivatives of GPI-2350 harbouring open inositol-monophosphate instead of cIP, 2-deoxy-2-fluoro-*scyllo*-inositol-1-*O*-dodecyl-phosphonic acid (GPI-1793) and *myo*-inositol-1-*O*-dodecylphosphonic acid methylester (GPI-2349), exerted low and very low inhibition, respectively, on the adipocyte GPI-PLC at the highest concentration tested, only, but blocked the bacterial and trypanosomal (G)PI-PLC with similar high potencies (Table 1) as reported previously [59,60]. These findings argue for some similarity in the catalytic mechanism involving the formation of stable or transient 1,2-cyclic phosphate bonds, but also for some differences in substrate recognition between the bacterial, trypanosomal and adipocyte (G)PI-PLC. It would be interesting to know whether the cyclic phosphate bond of GPI-2350 is opened by the (G)PI-PLC. The reversibility of the interaction of GPI-2350 with the (G)PI-PLC is suggested by the observation that half-maximal inhibition of bacterial and trypanosomal (G)PI-PLC by GPI-2350 was completely abrogated upon 10-fold dilution of the reaction mixtures with buffer containing fresh GPI-protein substrate.

3.2. Blockade of insulin- and glimepiride-induced lipolytic cleavage of GPI-proteins by GPI-2350 in isolated DIGs and intact adipocytes

On the basis of the observed interference of GPI-2350 with cleavage of GPI-proteins by adipocyte GPI-PLC in vitro when both are presented in separate complexes (detergent micelles and DIGs, respectively), we next studied the effect of GPI-2350 on basal and stimulated GPI-PLC activity in intact adipocytes and isolated DIGs with exogenous or endogenous GPI-proteins as substrates

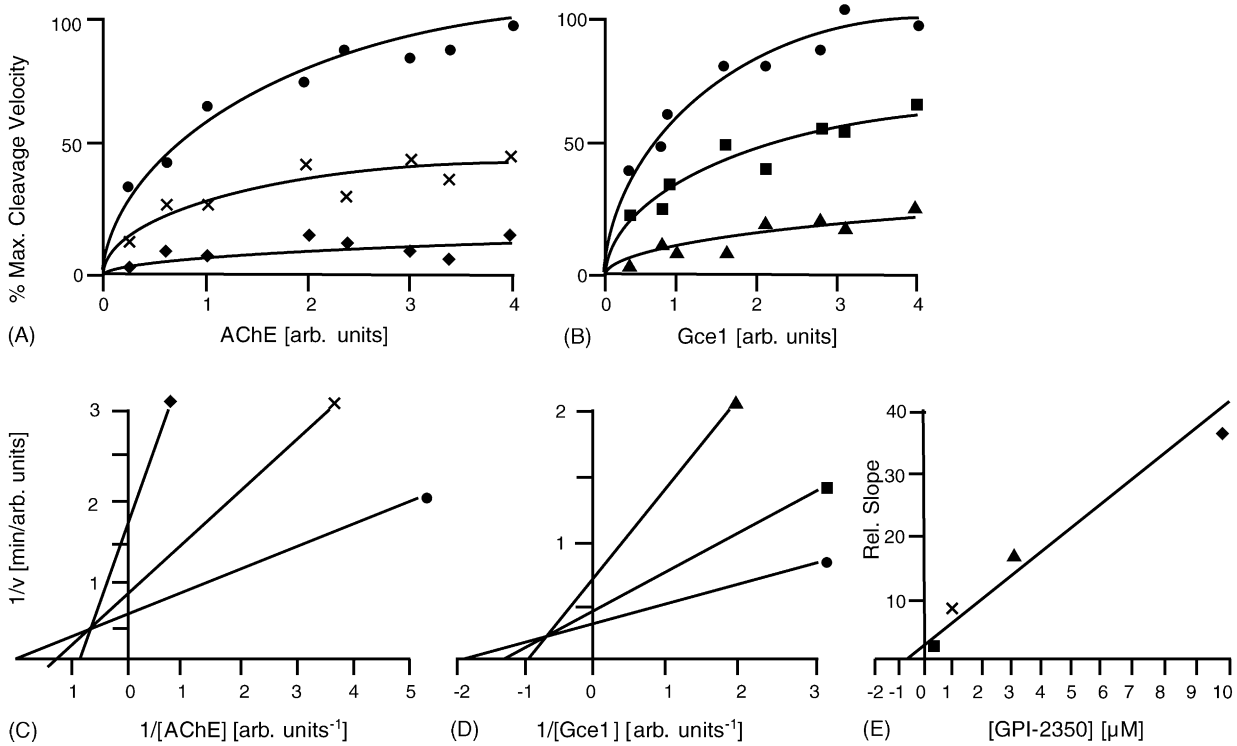

Fig. 3. Type of inhibition of adipocyte GPI-PLC by GPI-2350. (A–D) hcDIGs prepared from untreated rat adipocytes were incubated (1 h, 25 °C) with increasing amounts of partially purified bovine AChE (panels A and C) or [^{14}C]inositol-labelled yeast Gce1 (panels B and D; see Section 2) in the presence of 0.1% TX-100 in the absence (●) or presence of 0.3 (■), 1 (×), 3 (▲) and 10 (◆) μM GPI-2350 and then subjected to TX-114 partitioning. The relative amounts of hydrophilic AChE and Gce1 were determined by assaying the aqueous phases for AChE activity and radioactivity, respectively. Means from three independent incubations and partitionings with activity and radioactivity measurements in quadruplicate, each, are given. The relative cleavage velocity (maximum set at 100%) was plotted vs. the relative concentration of AChE (arb. units according to total activity) or Gce1 (arb. units according to total radioactivity) contained in the incubation mixture prior to partitioning. Data were fitted according to Michaelis-Menten (panels A and B) and Lineweaver–Burk (panels C and D) equations using the program Origin. (E) The K_i for GPI-2350 was determined by plotting the slopes of the four individual Lineweaver–Burk plots from the K_m measurements for AChE and Gce1 at various inhibitor concentrations against the four different GPI-2350 concentrations used. On the basis of the very similar apparent K_m values calculated for AChE and Gce1 (see panels C and D; absence of inhibitor), the slopes obtained for the various inhibitor concentrations and GPI-proteins were used in a single plot, representative for a typical GPI-protein substrate. The slope of the resulting plot corresponds to $(K_m/V_{max}) + ([I]K_m/K_iV_{max})$, where $[I]$ is the concentration of GPI-2350. A linear regression for the values provides $-K_i$ as the intersection with the x-axis, where the slope is zero.

(Fig. 5). In isolated rat adipocytes, the GPI-PLC activity monitored as amphiphilic-to-hydrophilic conversion of endogenous 5′-Nuc/Gce1/aP in course of their cleavage was increased by up to 5.3 ± 1.4/3.4 ± 0.9/2.9 ± 1.0 in response to glimepiride and 2.9 ± 1.3/3.1 ± 1.2/2.5 ± 1.5 in response to insulin; Fig. 5(E and G). The stimulation was partially maintained in hcDIGs prepared from the glimepiride- and insulin-pretreated adipocytes (3.2 ± 0.6- and 1.7 ± 0.4-fold, respectively, for 5′-Nuc, Fig. 5C; 2.5 ± 0.7 and 2.2 ± 0.4 for Gce1, 3.5 ± 0.9 and 3.1 ± 0.8 for aP). Remarkably, the GPI-PLC was activated (up to 3.9 ± 1.3-fold for 5′-Nuc, Fig. 5A; 2.6 ± 0.5 for Gce1 and 3.1 ± 1.2 for aP) upon direct incubation of hcDIGs prepared from untreated adipocytes with glimepiride but not insulin (Fig. 5A). In intact adipocytes activation of the GPI-PLC seems to be more pronounced for glimepiride than for insulin (Fig. 5E and G). GPI-2350 reduced the basal as well as glimepiride- and insulin-stimulated GPI-PLC

Table 1
Characteristics of the (G)PI-PLC inhibitors

	GPI-2350		GPI-1793		GPI-2349	
	IC_{50} (μM)	Inhibition % at 1 mM	IC_{50} (μM)	Inhibition % at 1 mM	IC_{50} (μM)	Inhibition % at 1 mM
GPI-PLC adipocytes	0.2–0.5	95 ± 11	n.a.	42 ± 5	n.a.	27 ± 6
GPI-PLC *T. brucei*	2–5	85 ± 9	25–35	89 ± 7	310–390	66 ± 8
PI-PLC *B. cereus*	10–20	75 ± 8	110–140	70 ± 10	n.a.	24 ± 5

hcDIGs prepared from rat adipocytes, GPI-PLC from *T. brucei* and PI-PLC from *B. cereus* were incubated with solubilized and partially purified bovine erythrocyte AChE under appropriate conditions (see Section 2) in the absence or presence of up to 1 mM of the inhibitors indicated. Upon TX-114 partitioning, cleavage rates were calculated from the amount of hydrophilic AChE activity recovered with the TX-114-depleted phase. The apparent cleavage rates determined for control reactions lacking inhibitor and any source for the GPI-PLC were set at 0 and 100% inhibition, respectively. Means ± S.D. from at least three independent incubations with partitionings/AChE assays in quadruplicate, each, are given. n.a.: not applicable.

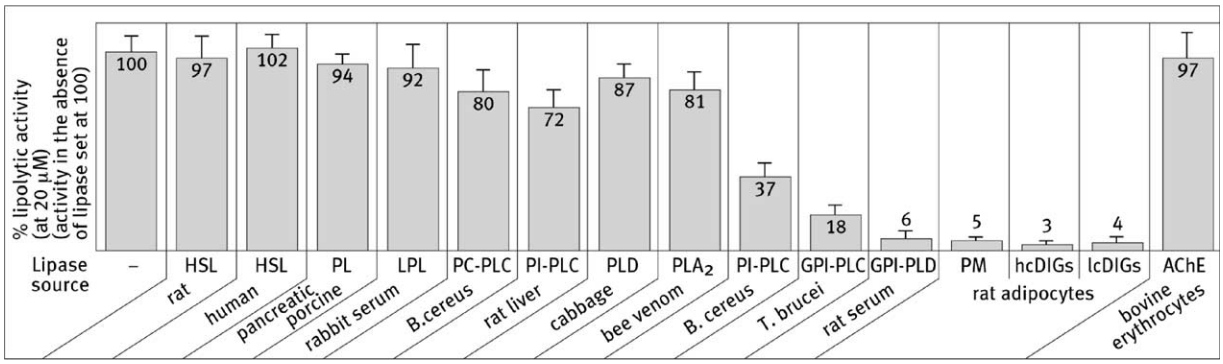

Fig. 4. Selectivity of GPI-2350. Various (partially) purified or recombinant lipases (HSL, PL, LPL, PC-PLC, PI-PLC, PLD, PLA_2, GPI-PLC, GPI-PLD) of different origin as indicated, bovine erythrocyte AChE as well as total PM, hcDIGs and lcDIGs from isolated rat adipocytes were assayed in the absence or presence of GPI-2350 (50 μM) according to typical assay protocols (see Section 2). Means ± S.D. of at least three independent incubations with measurements in duplicate, each, are given.

activity in concentration-dependent fashion to lower than basal and similar levels in both isolated hcDIGs and intact adipocytes (Fig. 5A–F). GPI-2350 did not abrogate activation of the GPI-PLC in response to insulin or glimepiride when the inhibitor was present prior to and during incubation of the intact adipocytes with either stimulus, but absent during subsequent assaying of the isolated and intensely washed hcDIGs (data not shown). This strongly argues for direct inhibition of the catalytic activity of the GPI-PLC by GPI-2350 rather than of its activation by the upstream insulin or glimepiride signalling cascades. The IC_{50} for inhibition of the GPI-PLC when assayed with intact adipocytes (5–10 μM, Fig. 5F) was higher compared to those for isolated intact hcDIGs (1 μM, Fig. 5B and D) as well as solubilized hcDIGs and PM (0.2–0.5 μM, Fig. 2). This is most easily explained by metabolic degradation of

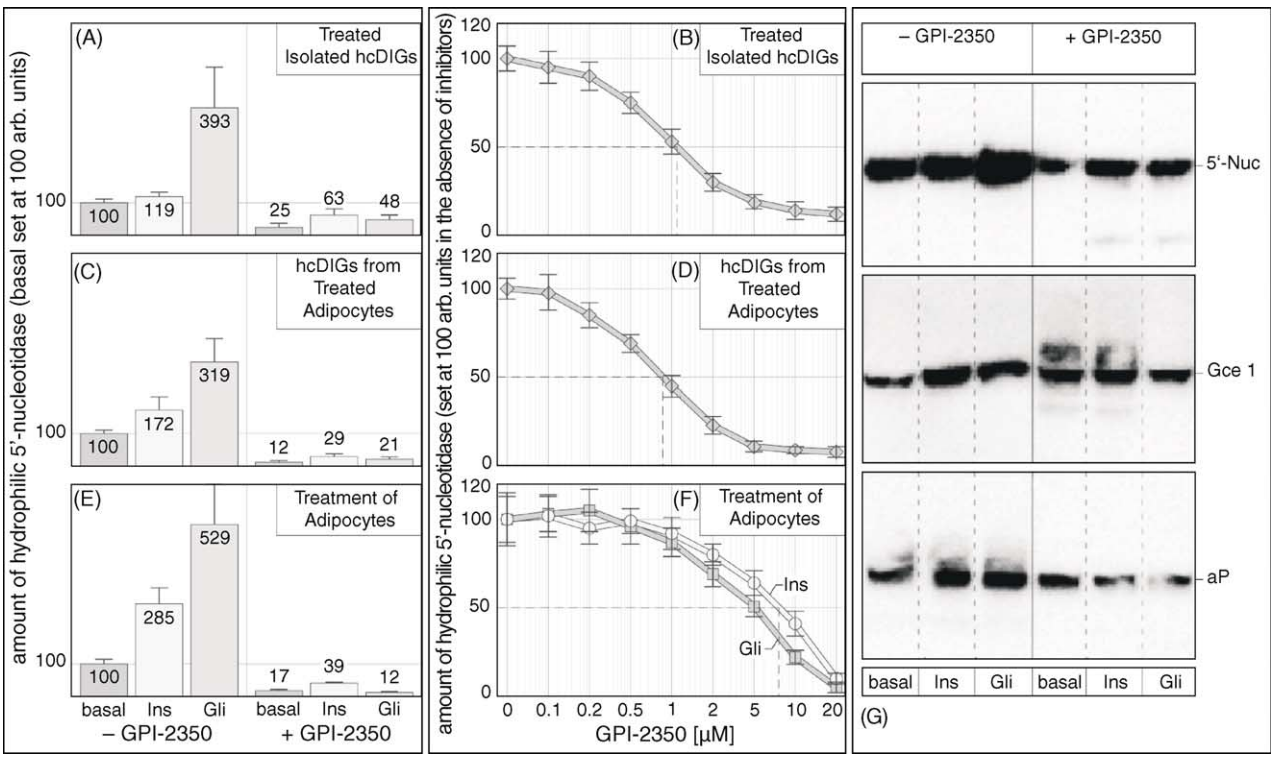

Fig. 5. Effect of GPI-2350 on cleavage of GPI-proteins by insulin-/glimepiride-induced GPI-PLC. (A and B) hcDIGs were prepared from untreated rat adipocytes and then incubated (5 min, 37 °C) in the absence or presence of GPI-2350 (panel A, 50 μM; panel B, increasing conc.) followed by treatment (2 h, 30 °C) without or with insulin (10 nM) or glimepiride (20 μM) as indicated. (C and D) Isolated rat adipocytes were incubated (15 min, 37 °C) in the absence or presence of insulin (10 nM) or glimepiride (20 μM) as indicated. hcDIGs were prepared and subsequently incubated (2 h, 30 °C) with GPI-2350 (panel C, 50 μM; panel D, increasing conc.). (E–G) Isolated rat adipocytes were incubated (5 min, 37 °C) in the absence or presence of GPI-2350 (panels E and G, 50 μM; Panel F, increasing conc.) and then treated (90 min, 37 °C) without or with insulin (10 nM) or glimepiride (20 μM) as indicated. hcDIGs were prepared. (A–D) Hydrophilic 5′-Nuc recovered with the TX-114-depleted phase was determined by activity measurement. (E–G) Proteins recovered with the TX-114-depleted phase of hcDIGs were analyzed for hydrophilic 5′-Nuc (by immunoblotting) and Gce1 (by photoaffinity-labelling). Means ± S.E. of three independent cell incubations with activity measurements and gel runs in duplicate (representative one shown) each, are given.

GPI-2350, such as spontaneous or enzymic decyclization, upon incubation with intact adipocytes.

Under the experimental conditions used for the isolation of DIGs and PM, the majority of the GPI-PLC total activity in the PM was recovered with hcDIGs compared to lcDIGs and non-DIG areas along with major portions of the typical DIGs marker protein, caveolin-1, and the DIGs resident proteins, p115, aP, 5′-Nuc and Gce1 (Table 2). Since isolated hcDIGs are characterized by a considerably lower protein content than lcDIGs and non-DIG areas, the GPI-PLC is enriched by 5-, 3.5- and 15-fold in hcDIGs versus total PM, lcDIGs and non-DIG areas, respectively, consistent with its colocalization with GPI-protein substrates at hcDIGs in the PM of rat adipocytes.

3.3. Dependence of the redistribution of GPI-anchored and acylated signalling proteins within DIGs on GPI-PLC activation in rat adipocytes

We next investigated whether inhibition of the adipocyte GPI-PLC affects the localization and the recently described [34,40] stimulus-induced redistribution of GPI-anchored as well as acylated signalling proteins within DIGs of the adipocyte PM. For this, hc/lcDIGs were prepared from adipocytes which had been incubated in the absence or presence of GPI-2350 prior to challenge with glimepiride and then analyzed for the presence of several GPI-anchored or acylated signalling proteins (Fig. 6). Glimepiride-induced a robust redistribution of pp59^{Lyn}, Gce1 and 5′-Nuc from hcDIGs to lcDIGs as manifested in the 3- to 5-fold increases in their amounts at lcDIGs, which corresponded to the 70–90% losses at hcDIGs compared to basal adipocytes. This redistribution was almost completely abolished in the presence of max. effective concentration of GPI-2350. In contrast, the high expression of the hcDIGs resident proteins, caveolin-1 and IRβ, at hcDIGs versus lcDIGs as well as the similar expression of Glut4 at hcDIGs and lcDIGs [38], which was not significantly affected by glimepiride in each case (1.09 ± 0.18 for caveolin, 0.72 ± 0.21 for IRβ, 1.44 ± 0.39 for Glut4), did not change significantly in the presence of GPI-2350 (1.43 ± 0.29 for caveolin, 0.79 ± 0.33 for IRβ, 1.38 ± 0.25 for Glut4; Fig. 6). This demonstrates that potent inhibition of the GPI-PLC specifically interferes with the stimulus-induced translocation of a subset of GPI-anchored and acylated signalling proteins, such as Gce1 and pp59^{Lyn}, from hcDIGs to lcDIGs rather than causes general and unspecific changes in the structure of DIGs.

Heterogeneity of DIGs in terms of their protein and lipid composition has been described previously on the basis of differential solubilization of certain membrane proteins by non-ionic detergents of varying hydrophilic–lipophilic balance [62]. The transmembrane protein, prominin, was found to be soluble in TX-100 but insoluble in Lubrol-WX in the apical plasma membrane domain of MDCK cells in contrast to the GPI-protein, placental aP, which resisted solubilization by both detergents. This suggests the existence of separate ‘‘TX-100-’’ and ‘‘Lubrol-WX-’’ DIGs in polarized epithelial cells, which in rat adipocytes may correspond to hcDIGs and lcDIGs, respectively. Consequently, we next compared in adipocytes the distribution and the putative glimepiride-induced (GPI-PLC-dependent) redistribution of the DIGs-resident signalling proteins (5′-Nuc, Gce1, pp59^{Lyn}) between ‘‘TX-100-’’ and ‘‘Lubrol-WX-’’ DIGs separated by sucrose gradient centrifugation (Fig. 7).

In the basal state, 5′-Nuc, Gce1 and pp59^{Lyn} were predominantly recovered (rel. amount per fraction volume) with ‘‘TX-100-hcDIGs’’ floating at low buoyant density (0.5–0.65 M sucrose) on top of the gradient (fractions 3 + 4). In contrast, upon solubilisation with Lubrol-WX, these proteins were distributed about equally between high and low buoyant density-floating lc/hcDIGs (fractions 3–6). Treatment of adipocytes with glimepiride led to a significant enrichment of 5′-Nuc, Gce1 and pp59^{Lyn} in TX-100- as well as Lubrol-WX-insoluble high buoyant density lcDIGs (fractions 5 + 6) with only residual amounts left with low buoyant density hcDIGs (fractions 3 + 4). This glimepiride-induced redistribution of DIG components was counteracted by GPI-2350 (Fig. 7). Both glimepiride and GPI-2350 did not significantly affect the low and moderate portions of 5′-Nuc, Gce1 and pp59^{Lyn} in the soluble fractions (7 + 8) and pellet fractions, respectively, using both detergents for the DIGs preparation.

Table 2
Distribution of the GPI-PLC and typical DIGs resident proteins within the adipocyte PM

	Rel. GPI-PLC activity		Rel. protein amounts				
	Total	Specific	Caveolin	p115	aP	5′-Nuc	Gce1
PM	100 ± 21	100 ± 12	100 ± 27	100 ± 35	100 ± 21	100 ± 15	100 ± 41
hcDIGs	57 ± 9	488 ± 117	64 ± 10	50 ± 19	81 ± 16	69 ± 23	91 ± 26
lcDIGs	25 ± 7	141 ± 38	20 ± 5	16 ± 9	33 ± 9	12 ± 8	38 ± 14
Non-DIG areas	11 ± 5	29 ± 13	8 ± 4	13 ± 6	5 ± 3	10 ± 4	4 ± 4

Total PM, hcDIGs, lcDIGs and non-DIG areas were prepared from isolated untreated rat adipocytes and assayed for GPI-PLC activity (measured as amphiphilic-to-hydrophilic conversion of exogenous AChE upon TX-114 partitioning), as well as for the amounts of caveolin-1 (determined by immunoblotting), p115 (determined by binding of synthetic PIG-41), aP, 5′-Nuc (determined by activity measurement) and Gce1 (determined by binding of cAMP) prior to TX-114 partitioning. The total and specific activities of the GPI-PLC as well as the relative amounts of the GPI-proteins recovered with the PM were set at 100 arb. units in each case. Means ± S.D. of three independent preparations with measurements in triplicate, each, are given.

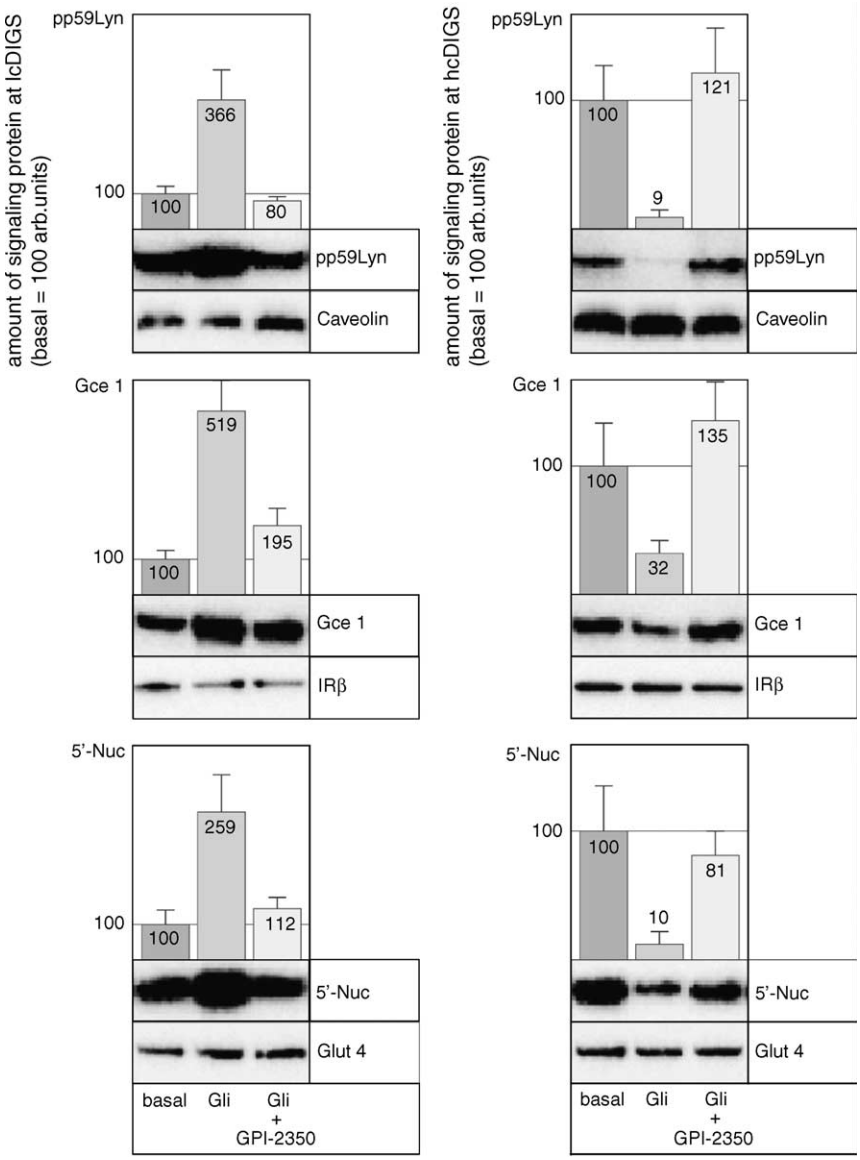

Fig. 6. Effect of GPI-2350 on the glimepiride-induced redistribution of signalling proteins within hc/lcDIGs. Isolated rat adipocytes were treated (5 min, 37 °C) without or with GPI-2350 (50 μM final conc.) and then incubated (120 min, 37 °C) in the absence (basal) or presence of glimepiride (20 μM) as indicated. hcDIGs and lcDIGs were prepared and assayed for the presence of $pp59^{Lyn}$, 5′-Nuc, caveolin-1, IRβ, Glut4 (by immunoblotting) and Gce1 (by photoaffinity-labelling). The amount of $pp59^{Lyn}$, Gce1 and 5′-Nuc recovered with hc/lcDIGs is given relative to the control reaction in the absence of GPI-2350 (basal set at 100). Means ± S.D. of at least three independent cell incubations with gel runs in duplicate (representative one shown) each, are given.

The unaltered relative distribution of the IR as well as cholesterol excludes gross structural changes of the adipocyte PM in response to either treatment (Fig. 7). In conclusion, the use of TX-100 and Lubrol-WX for solubilization of isolated PM confirmed the existence of (at least) two distinct subspecies of DIGs in rat adipocytes, one insoluble in TX-100 (and Lubrol-WX) exhibiting low buoyant density and high cholesterol content (= hcDIGs), and the other one soluble in TX-100 but insoluble in Lubrol-WX exhibiting high buoyant density and low cholesterol content (= lcDIGs). Remarkably, glimepiride apparently induces (in GPI-PLC-dependent fashion) the generation of a third subspecies of DIGs, insoluble in both detergents and of the same high buoyant density/low cholesterol content as characteristic for the TX-100-soluble/Lubrol-WX-insoluble ones expressed in the absence of glimepiride (and therefore with these collectively termed as lcDIGs). Consequently, TX-100 insolubility in combination with high buoyant density/low cholesterol content, but not insolubility in Lubrol-WX per se, seems to be sufficient for biochemical characterization and functional analysis of lcDIGs and was used in the following.

We next studied whether the lipolytically cleaved and/or uncleaved GPI-proteins are translocated to lcDIGs in isolated rat adipocytes upon activation of the GPI-PLC. For this, cells were incubated in the absence or presence of GPI-2350 and then challenged with insulin or glimepiride. The portions of hydrophilic and amphiphilic versions of

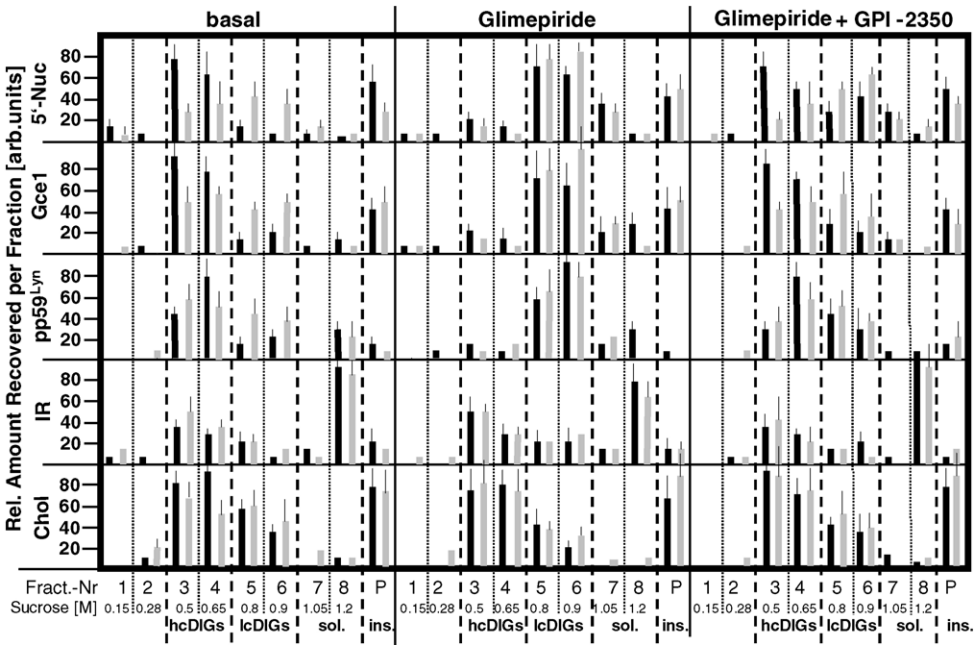

Fig. 7. Effect of GPI-2350 on the glimepiride-induced redistribution of signalling proteins within DIGs of different detergent sensitivity. Isolated rat adipocytes were treated (5 min, 37 °C) without or with GPI-2350 (50 μM final conc.) and then incubated (2 h, 37 °C) in the absence or presence of glimepiride (20 μM) as indicated. Isolated PM pellets (200 μg) were suspended in 200 μl of 50 mM Tris/HCl (pH 7.5), 1 mM EGTA, 150 mM NaCl containing protease inhibitors and either 0.5% Lubrol-WX (grey bars) or 1% TX-100 (black bars) and then incubated (30 min, 4 °C). The detergent lysates were adjusted to 1.2 M sucrose using 2.4 M sucrose in the same buffer, placed at the bottom of SW60 tubes and overlaid with 1 ml of 0.9 M, 0.5 ml of 0.8 M, 1 ml of 0.7 M and 1 ml of 0.1 M sucrose. After centrifugation (300,000 × *g*, 16 h, 4 °C), 500 μl fractions (1–8) were collected from the top to the bottom of the gradient. 400-μl portions were precipitated by the addition of 1 ml ice-cold TCA and incubation (15 min, 4 °C). After centrifugation (16,000 × *g*, 5 min), the pellets were washed two times with acetone, dissolved in sample buffer, as was done directly with the gradient pellet (P), and then analysed by SDS-PAGE followed by immunoblotting for 5′-Nuc, Gce1, $pp59^{Lyn}$, and IR. 50-μl portions were analysed for cholesterol by TLC. The maximal amount of protein/cholesterol recovered with a given fraction was set at 100 arb. units in each case. Means ± S.D. of three independent cell incubations with gel runs in duplicate each are given. According to the buoyant density, fractions 3 + 4 contain hcDIGs, fractions 5 + 6 contain lcDIGs, fractions 7 + 8 contain soluble proteins (sol.) and the pellet contains detergent-insoluble material (ins.).

the GPI-proteins, 5′-Nuc, aP and Gce1, recovered with total PM, hcDIGs and lcDIGs were determined by TX-114 partitioning (Fig. 8). Treatment with insulin and more potently glimepiride caused the generation of hydrophilic GPI-proteins in the PM, which was completely blocked by GPI-2350 demonstrating efficient GPI-PLC inhibition. In response to both insulin and glimepiride, the increases in the amounts of hydrophilic 5′-Nuc, aP and Gce1 were detected at hcDIGs, but not lcDIGs, and found to be accompanied by decreases in the amphiphilic versions at hcDIGs but not lcDIGs. These changes were reversed to even below basal values in the presence of GPI-2350 demonstrating the lipolytic nature of this amphiphilic-to-hydrophilic conversion (Fig. 8). Thus, hydrophilic GPI-proteins generated by the insulin-/glimepiride-induced GPI-PLC at hcDIGs remain associated with hcDIGs *via* a molecular mechanism not relying on the GPI anchor. Interestingly, the pronounced glimepiride-induced redistribution of 5′-Nuc, Gce1 and aP from hcDIGs to lcDIGs (see Fig. 6), which was completely eliminated by GPI-2350, was restricted to their uncleaved versions (Fig. 8). This was reflected in the 2.5- to three-fold elevated levels in the amphiphilic but unaltered low levels in the hydrophilic GPI-proteins recovered with lcDIGs. Similarly, the moderate insulin-induced accumulation of 5′-Nuc, Gce1 and aP at lcDIGs, sensitive to inhibition by GPI-2350, was restricted to the amphiphilic versions. All three GPI-proteins studied displayed the correlation between stimulus-induced lipolytic cleavage at hcDIGs and redistribution of their amphiphilic uncleaved versions to lcDIGs, exclusively, with only minor differences in efficacy (Fig. 8). This argues for a causal relationship between GPI-PLC activation, accumulation of lipolytically cleaved GPI-proteins at hcDIGs, and redistribution of intact GPI-proteins from hcDIGs to lcDIGs.

3.4. Blockade of the regulated dissociation of GPI-anchored and acylated signalling proteins from caveolin by inhibition of the GPI-PLC

The redistribution of signalling proteins from hcDIGs to lcDIGs in rat adipocytes has recently been shown to be accompanied by their dissociation from caveolin-1 and activation [40,63]. We next investigated the putative causal relationship between dissociation from caveolin/activation and stimulus-induced lipolytic cleavage of GPI-proteins in rat adipocytes by inhibiting GPI-PLC and subsequent analysis of the interaction with caveolin-1 of Gce1 and

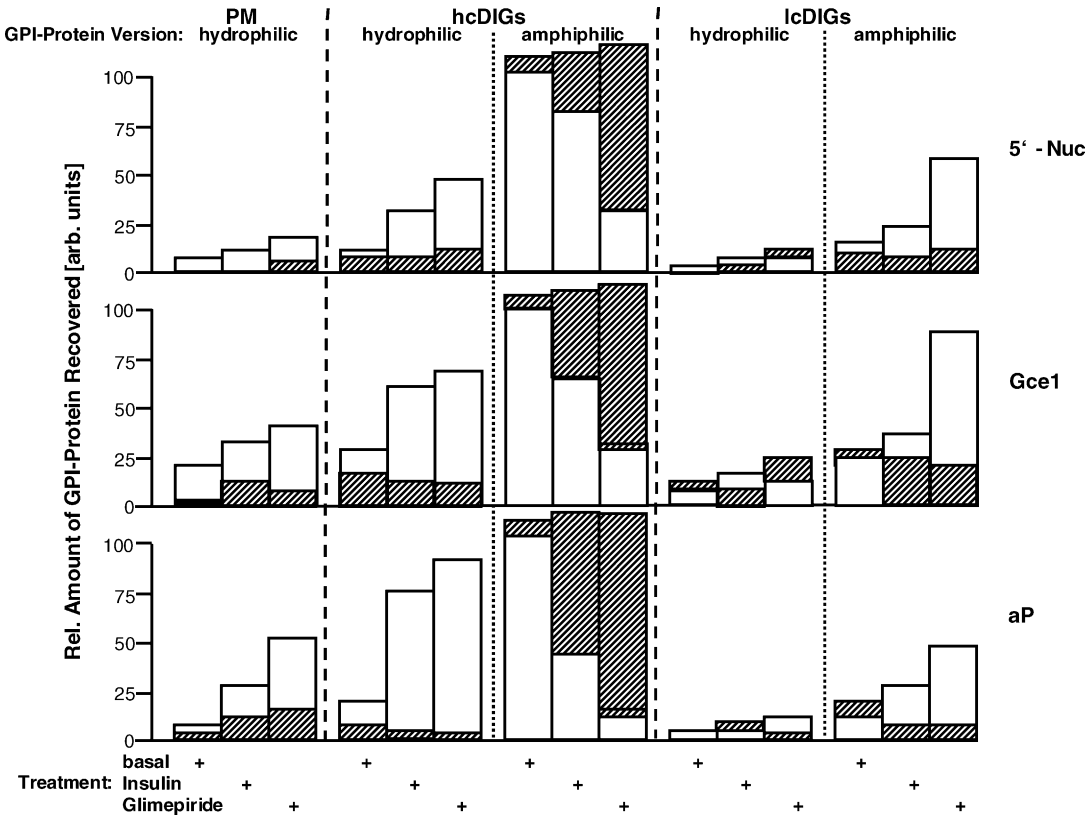

Fig. 8. Effect of insulin, glimepiride and GPI-2350 on the redistribution of amphiphilic and hydrophilic GPI-proteins within the adipocyte PM. Isolated rat adipocytes were treated (5 min, 37 °C) without (open bars) or with GPI-2350 (50 μM, hatched bars) and then incubated (2 h, 37 °C) in the absence or presence of glimepiride (20 μM) or insulin (10 nM) as indicated. Total PM, hcDIGs and lcDIGs were prepared and then subjected to TX-114 partitioning. The TX-114-enriched and depleted phases were assayed for 5′-Nuc (by activity measurement) and Gce1 (by photoaffinity-labelling). The amounts of amphiphilic and hydrophilic GPI-protein were calculated relative to the amphiphilic version in hcDIGs prepared from basal adipocytes in the absence of GPI-2350 (set at 100 arb. units each). The recoveries of the hydrophilic and amphiphilic GPI-proteins from hcDIGs *plus* lcDIGs were comparable under the various incubation conditions. Means of at least three independent cell incubations with activity measurements/gel runs in duplicate, each, are given. S.D. values were within ± 30% in each case and typically ± 10–15%.

$pp59^{Lyn}$ as well as kinase activity of the latter (Fig. 9). The insulin- (35–45%) and glimepiride- (75–85%) induced maximal losses of both $pp59^{Lyn}$ and Gce1 from caveolin-1 immunoprecipitates prepared from isolated and solubilized hcDIGs were completely abrogated by GPI-2350 (50 μM; Fig. 9A) with IC_{50} of 5–10 μM (Fig. 9B). This potency is similar to GPI-PLC inhibition by GPI-2350 in intact adipocytes (Fig. 5). Binding of the CSD of caveolin-1 to the CBD of signalling proteins, such as non-receptor tyrosine kinases, and conversely, relief of the CSD from binding to the CBD have been shown in many but not all cases to trigger inactivation and activation, respectively, of the signalling proteins in in vitro assays [64,65]. This implies a regulatory function of the CSD–CBD interaction in signal transduction operating at plasma membrane DIGs [37,66,67]. The possibility of specific interference with the dissociation of GPI-anchored and acylated signalling proteins from caveolin *via* inhibition of the GPI-PLC enabled us to test this so-called ''caveolin-signalling hypothesis'' [67] for insulin and glimepiride signal transduction in intact cells. For this, cytosolic fractions and lcDIGs prepared from rat adipocytes, which had been treated with GPI-2350 prior to challenge with insulin or glimepiride, were probed for tyrosine phosphorylation of lcDIGs-associated $pp59^{Lyn}$ and one of its substrates, cytosolic IRS-1, respectively (Fig. 10). The robust tyrosine phosphorylation of both IRS-1 and $pp59^{Lyn}$ in response to glimepiride was reduced by GPI-2350 to almost basal levels in concentration-dependent fashion (IC_{50} = 5–20 μM). Thus, the glimepiride-induced dissociation from caveolin and activation of $pp59^{Lyn}$ depends on the function of the GPI-PLC. This finding is compatible with a negative effect of binding of the CSD to the CBD of DIGs-associated $pp59^{Lyn}$ in intact rat adipocytes. In contrast, the tyrosine phosphorylation of IRS-1 and $pp59^{Lyn}$ in response to insulin, which was more and less potent, respectively, compared to glimepiride was not significantly affected by GPI-2350 (Fig. 10). This suggests that (i) the moderate insulin-induced activation of $pp59^{Lyn}$ does not depend on its (GPI-PLC-mediated) dissociation from caveolin-1 and (ii) the dramatic insulin-induced tyrosine phosphorylation of IRS-1 does not rely on the (GPI-PLC-independent) stimulation of $pp59^{Lyn}$, but rather is predominantly due to activation of the IR tyrosine kinase.

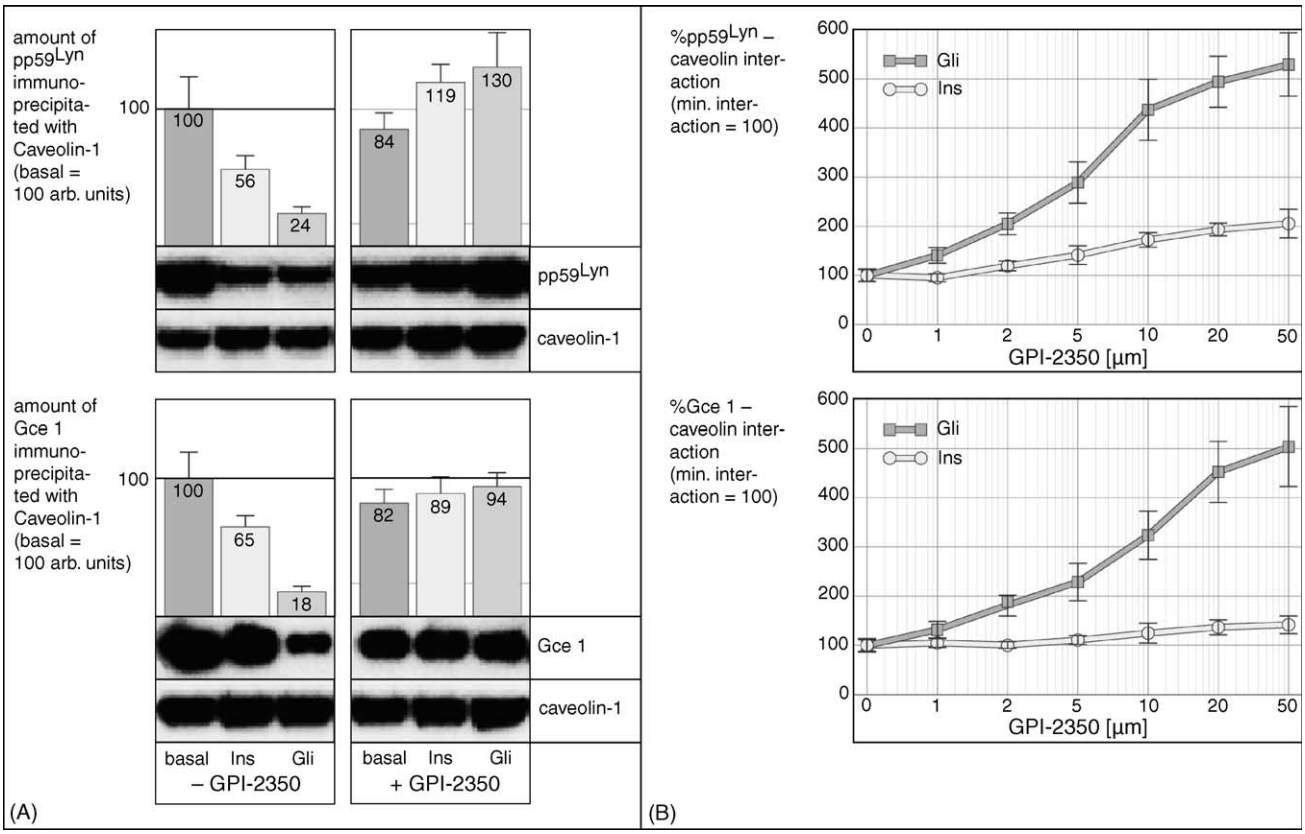

Fig. 9. Effect of GPI-2350 on the glimepiride-/insulin-induced dissociation of pp59^{Lyn} and Gce1 from caveolin. Isolated rat adipocytes were treated (5 min, 37 °C) without or with GPI-2350 (left panels, 50 μM; right panels, increasing conc.) and then incubated (2 h, 37 °C) in the absence or presence of insulin (10 nM) or glimepiride (20 μM). hcDIGs were prepared from the adipocytes, solubilized and then subjected to immunoprecipitation of caveolin-1. The caveolin-1 immunoprecipitates were assayed for the presence of pp59^{Lyn} and Gce1 by immunoblotting and photoaffinity-labelling, respectively. The amount of pp59^{Lyn} and Gce1 is given relative to the absence of GPI-2350 in the control reaction (panel A, basal set at 100) or in the insulin-/glimepiride-stimulated state (panel B, set at 100) after correction for the recovery of immunoprecipitated caveolin-1 by homologous immunoblotting (see gel insets). Means ± S.D. of at least four independent cell incubations with gel runs in duplicate (representative one shown) each, are given.

3.5. Downregulation of the insulin-mimetic metabolic activity of glimepiride by inhibition of the GPI-PLC

Next we studied whether the differential effects of GPI-PLC inhibition on IRS-1 tyrosine phosphorylation in response to glimepiride and insulin are reflected in their metabolic activity in insulin target cells. For this, isolated rat adipocytes were pretreated with GPI-2350 prior to challenge with either stimulus and then assayed for glucose transport and isoproterenol-induced lipolysis (Fig. 11). The stimulation of glucose transport and inhibition of isoproterenol-induced lipolysis by glimepiride were impaired in the presence of GPI-2350 in concentration-dependent fashion (IC_{50} = 2–5 μM; Fig. 11B) to lower than control values (at 50 μM, Fig. 11A). Consequently, the glimepiride concentration–response curves were shifted to the right in course of half-maximal inhibition of the GPI-PLC by GPI-2350 (5 μM) compared to the absence of inhibitor, whereas complete inhibition (50 μM) was accompanied by complete blockade of the glimepiride responses (Fig. 11C). In contrast, insulin stimulation of glucose transport and insulin inhibition of isoproterenol-induced lipolysis, being 2.5- to 3.5-fold more pronounced compared to glimepiride, were reduced by GPI-2350 (50 μM) by 25 and 39%, respectively, only (Fig. 11A and B). These differential effects of GPI-PLC inhibition by GPI-2350 on the blockade of isoproterenol-induced lipolysis by glimepiride and insulin were confirmed by analysis of the release of NBD-FA from rat adipocytes (data not shown) prelabelled with this fluorescent fatty acid derivative [51]. Inhibitors of rat liver PI-PLC and bee venom PLA_2 failed to significantly affect basal and glimepiride-regulated glucose transport and lipolysis (Fig. 11A) arguing that GPI-2350 affects insulin-mimetic metabolic activity in rat adipocytes specifically by inhibition of the GPI-PLC.

Finally, we investigated the putative involvement of the GPI-PLC in signalling pathways of insulin-mimetic stimuli other than glimepiride, which are either dependent on or independent of the redistribution of GPI-proteins within DIGs [34]. In rat adipocytes, disruption of hcDIGs by cholesterol depletion using m-β-CD [38], inactivation of the PIG receptor, p115, by trypsin-/NaCl- or NEM-treatment [41] or occupancy of p115 with the synthetic ligand, PIG-41 [40,63], led to pronounced increases in the amount

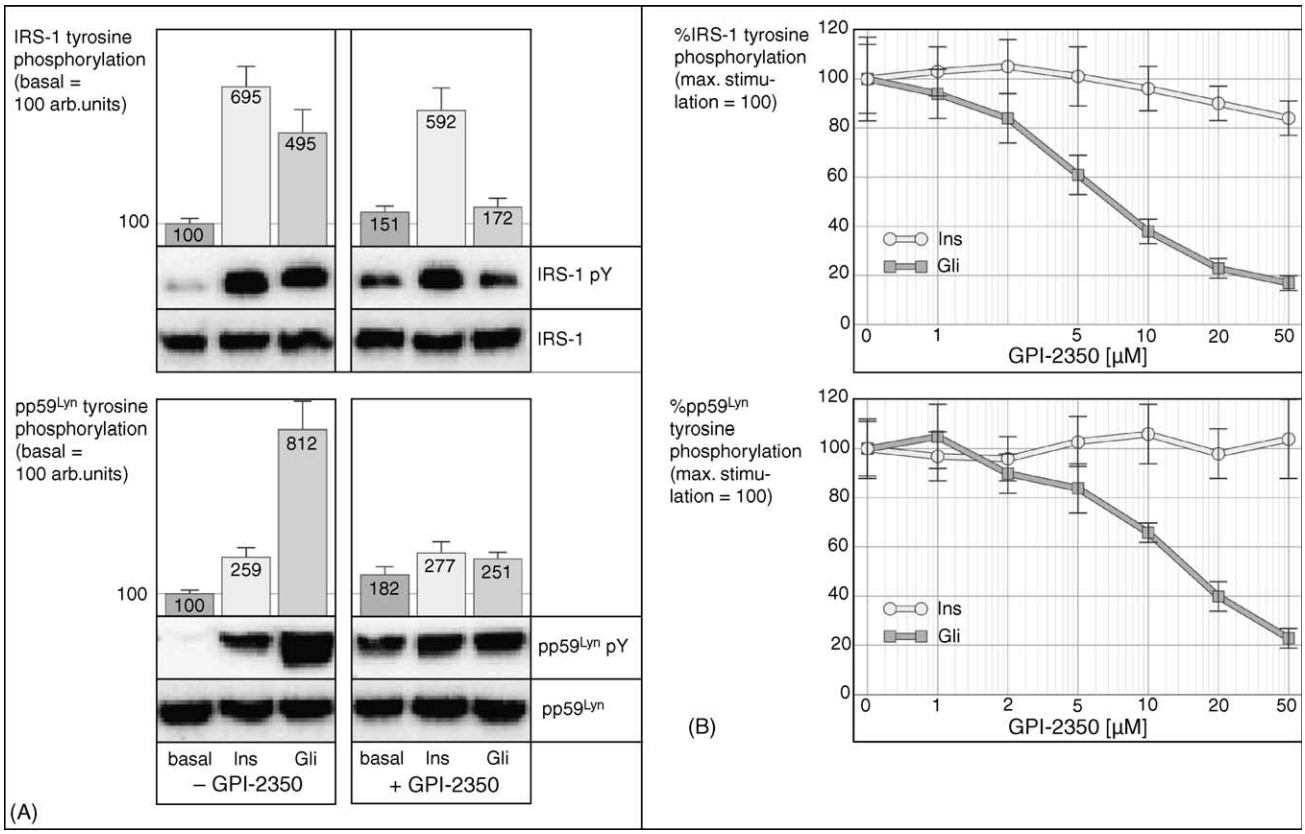

Fig. 10. Effect of GPI-2350 on the glimepiride-/insulin-induced tyrosine phosphorylation of IRS-1 and pp59^{Lyn}. Isolated rat adipocytes were treated (5 min, 37 °C) without or with GPI-2350 (panel A, 50 μM; panel B, increasing conc.) and then incubated (2 h, 37 °C) in the absence or presence of insulin (10 nM) or glimepiride (20 μM). Cytosolic fraction (= defatted postnuclear infranatant; see Section 2) and lcDIGs were prepared and then used for immunoprecipitation of IRS-1 and pp59^{Lyn}. The immunoprecipitates were immunoblotted for phosphotyrosine. The amount of tyrosine-phosphorylated IRS-1 and pp59^{Lyn} is given relative to the absence of GPI-2350 in the control reaction (panel A, basal set at 100) or in the insulin-/glimepiride-stimulated state (panel B, set at 100 in each case) after correction for the recovery of immunoprecipitated IRS-1 and pp59^{Lyn} by homologous immunoblotting (see gel insets). Means ± S.D. of at least four independent cell incubations with gel runs in duplicate (representative one shown) each, are given.

of 5′-Nuc at lcDIGs and glucose transport activation (Table 3). In contrast, sodium orthovanadate as well as a synthetic peptide (CBDP) corresponding to the CBD stimulated glucose transport and IRS-1 tyrosine phosphorylation (data not shown) without concomitant induction of 5′-Nuc translocation to lcDIGs and even in the presence of GPI-2350. This is in agreement with their modes of action independent or downstream of the GPI-PLC, inhibition of IR and IRS-1 dephosphorylation by the tyrosine phosphatase inhibitor, vanadate [68], and the direct stimulation of pp59^{Lyn} leading to IRS-1 tyrosine phosphorylation by the CBDP [42].

Table 3
Effect of GPI-2350 on the translocation of 5′-Nuc and glucose transport induced by various insulin-mimetic stimuli in rat adipocytes

	Increase in 5′-Nuc activity at lcDIGs (basal set at 100 arb. units)		Glucose transport (basal set at 100 arb. units)	
	−GPI-2350	+GPI-2350	−GPI-2350	+GPI-2350
m-β-CD	595 ± 128	539 ± 104	289 ± 13	249 ± 18
CBDP	128 ± 41	107 ± 59	468 ± 37	515 ± 49
PIG-41	773 ± 195	894 ± 201	1264 ± 91	1195 ± 79
Sodium orthovanadate	93 ± 38	105 ± 34	707 ± 51	673 ± 45
Trypsin/NaCl	461 ± 92	530 ± 102	361 ± 40	313 ± 29
NEM	292 ± 60	319 ± 52	308 ± 33	288 ± 40

Isolated rat adipocytes were incubated in the absence (basal) or presence of m-β-CD (10 mM, 50 min), CBDP (300 μM, electroporation, followed by washing and subsequent incubation for 30 min), PIG-41 (10 μM, 15 min), sodium orthovanadate (1 mM, 15 min), trypsin (10 μg/ml, 15 min followed by treatment with 0.5 M NaCl and subsequent washing) and NEM (1 mM, 5 min followed by addition of DTT). After further incubation (1 h, 37 °C) without or with GPI-2350 (50 μM), portions of the cells were assayed for 5′-Nuc activity at the isolated lcDIGs, other portions (after 15 min incubation at 37 °C) were assayed for glucose transport. The increases in 5′-Nuc activity at lcDIGs and glucose transport during the basal incubations were set at 100 arb. units. Means ± S.D. of at least three independent cell incubations with activity/transport measurements in triplicate, each, are given.

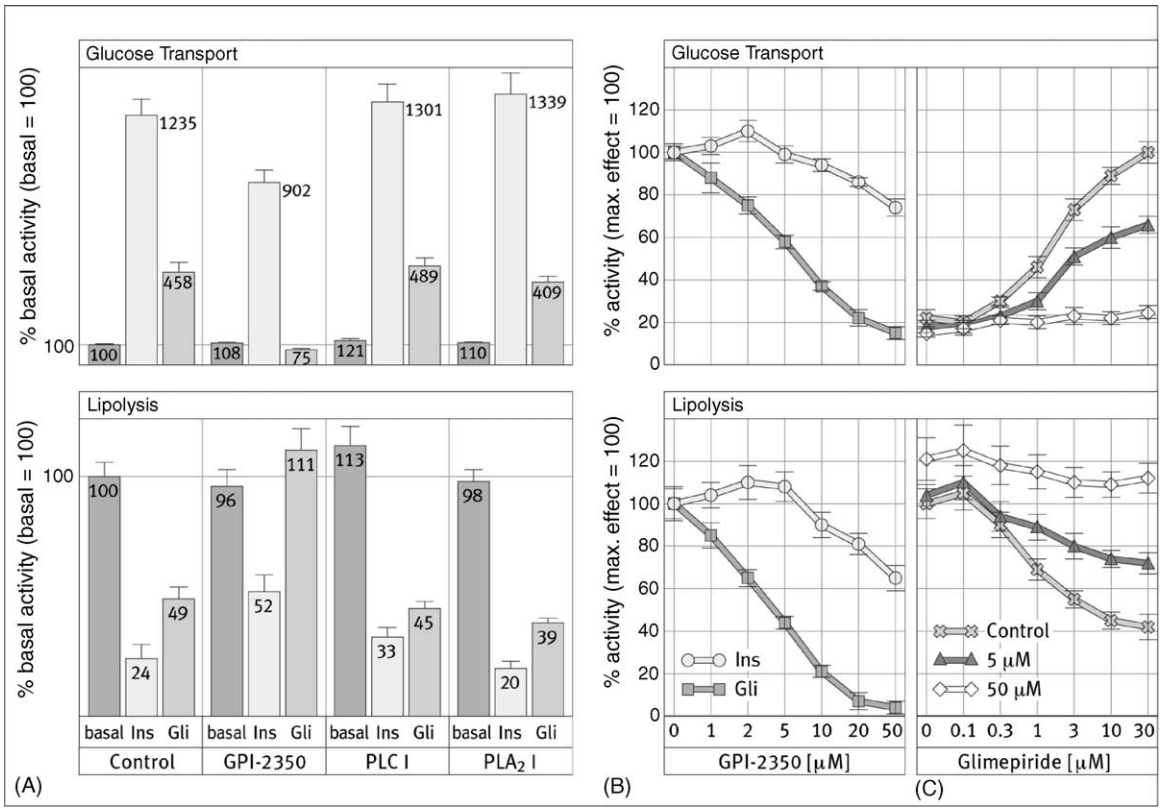

Fig. 11. Effect of GPI-2350 on the glimepiride-/insulin-induced metabolic activity. Isolated rat adipocytes were treated (5 min, 37 °C) without or with GPI-2350 (panel A, 50 μM; panel B, increasing conc.; panel C, 5 and 50 μM) and then incubated (15 min, 37 °C) in the absence or presence of insulin (Ins, 10 nM) or glimepiride (Gli, 20 μM or increasing conc.) as indicated. The adipocytes were then assayed for glucose transport and isoproterenol-induced lipolysis. The activity is given relative to the absence of GPI-2350 in the control reaction (panel A, basal) or in the insulin- and glimepiride-stimulated state (panels B and C, set at 100). Means ± S.D. of five independent cell incubations with activity measurements in triplicate, each, are given.

4. Discussion

4.1. GPI-PLC and glimepiride action

The apparent IC_{50} of GPI-2350 for counteracting stimulation of glucose transport and inhibition of lipolysis by glimepiride in isolated rat adipocytes is 2–5 μM (Fig. 11B) and thus correlates well with the inhibition of glimepiride-induced (i) tyrosine phosphorylation of $pp59^{Lyn}$ and IRS-1 (Fig. 10), (ii) relief of $pp59^{Lyn}$ from interaction with caveolin-1 at hcDIGs (Fig. 9), (iii) redistribution of uncleaved GPI-proteins (e.g. Gce1) and acylated $pp59^{Lyn}$ from hcDIGs to lcDIGs (Fig. 6), (iv) lipolytic cleavage of GPI-proteins by the GPI-PLC at hcDIGs (Fig. 5B and D), and (v) GPI-PLC activity when assayed with isolated PM, hcDIGs, or adipocytes and exogenous or endogenous GPI-protein substrates (Figs. 2 and 5). These correlations argue for a causal relationship between glimepiride activation of the GPI-PLC at hcDIGs and insulin-mimetic metabolic signalling in adipocytes. Interestingly, incubation of hcDIGs isolated from rat adipocytes with glimepiride causes activation of the GPI-PLC (Fig. 5A and B), which may be related to the described direct interaction of glimepiride with GPI lipids rather than with a putative proteinaceous receptor located at DIGs [33].

4.2. GPI-PLC and insulin action

Inhibition of the GPI-PLC in isolated rat adipocytes exerts only very moderate, albeit significant negative effects on insulin regulation of IRS-1 tyrosine phosphorylation, glucose transport and lipolysis (Figs. 10 and 11A). This partial impairment of insulin signalling and action by amphiphilic GPI-2350 is unlikely to be caused by unspecific membrane damage since the insulin-mimetic activity of vanadate was not impaired (Table 3). It seems unlikely that the blockade of the GPI-PLC exerted by 50 μM GPI-2350 is not sufficient for complete down-regulation of insulin signalling and action, since the glimepiride- and insulin-induced GPI-PLC activities were reduced to similar extent (Fig. 5E and F), yet only the glimepiride effects were abrogated (Figs. 10 and 11). Therefore, it is reasonable to assume that partial induction of the GPI-PLC by insulin in rat adipocytes has a function different from signalling to the insulin metabolic effector systems, albeit a role in their fine-tuning cannot be excluded so far. Insulin control of the cell surface expression of GPI-proteins *via* GPI anchor cleavage may represent (one of) the alternative function(s) of the GPI-PLC in insulin target cells.

4.3. Redistribution and activation of lipid-modified signalling proteins by GPI-PLC and insulin-mimetic stimuli

The present data can be combined with those from previous reports [30,34,38–40] leading to the following working hypothesis for signal generation in and transduction across the PM of rat adipocytes on the basis of the redistribution of lipid-modified signalling proteins, such as GPI-proteins and acylated tyrosine kinases, within DIGs (Fig. 12). Its key elements are the findings that (i) amphiphilic GPI-proteins with intact GPI anchor as well as hydrophilic GPI-proteins with lipolytically cleaved GPI anchor preferentially accumulate at hcDIGs versus lcDIGs (Fig. 7) and (ii) only uncleaved GPI-proteins redistribute from hcDIGs to lcDIGs in response to glimepiride and insulin (Figs. 6 and 8). Apparently, the GPI anchor functions as a signal for the recruitment to DIGs versus non-DIG areas, but does not determine the targeting to lcDIGs or hcDIGs. Consequently, an additional signal must be contained in GPI-proteins with intact or lipolytically cleaved GPI anchors for accumulation at hcDIGs. Its nature is unclear at present, but may reside within the PIG core structure identical in all GPI-proteins from yeast to man [1]. In fact, it has recently been demonstrated that lipolytically cleaved GPI-proteins are recognized by the trypsin-/NaCl- and NEM-sensitive PIG receptor protein, p115, which is located at hcDIGs of rat adipocytes [61]. It is tempting to speculate that this interaction is also involved in the targeting of intact GPI-proteins to hcDIGs, albeit their binding to p115 remains to be demonstrated. Our current working model (Fig. 12) implicates that the PIG core structure of the GPI anchor functions as the only hcDIGs-targeting signal (*via* recognition through p115) for a subset of GPI-proteins which are amenable to stimulus-induced redistribution to lcDIGs. In agreement with operation of the GPI-PLC upstream of p115, caveolin and $pp59^{Lyn}$, its inhibition by GPI-2350 does not block insulin-mimetic metabolic signalling in intact rat adipocytes in response to incubation with synthetic PIG-41, inactivation of p115, introduction of synthetic CBDP or cholesterol depletion (Table 3).

The present findings strongly suggest the expression of three distinct subspecies of DIGs in the PM of rat adipocytes: (i) TX-100- and Lubrol-WX-insoluble hcDIGs, (ii) TX-100-soluble and Lubrol-WX-insoluble lcDIGs in the basal state and (iii) TX-100- and Lubrol-WX-insoluble lcDIGs upon glimepiride challenge (Fig. 7). This is more compatible with the model of heterogenous DIGs rather than that of layered DIGs or homogenous DIGs with selective lipid extraction as has been recently proposed for their heterogenous structure as well as their biogenesis and maintenance [69]. Accordingly, layered DIGs are

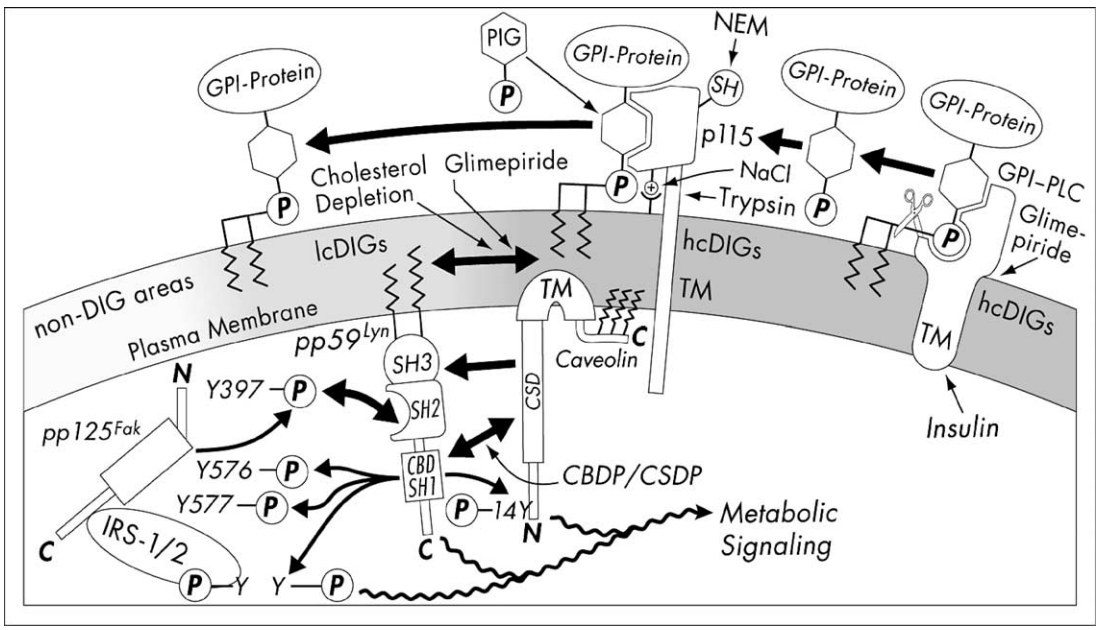

Fig. 12. Working model for the mechanism of redistribution of GPI-proteins between non-DIG areas, hcDIGs and lcDIGs within the adipocyte PM, its regulation by insulin, glimepiride and cholesterol depletion, the involvement of the GPI-PLC and the putative GPI-protein receptor, p115, and its coupling to downstream metabolic signalling to IRS-1 *via* caveolin, $pp125^{Fak}$ and $pp59^{Lyn}$. The topology, membrane orientation and type of anchorage at hcDIGs *via* transmembrane domains (TM) of the GPI-PLC and p115 is hypothetical. However, the active and binding sites, respectively, facing the extraplasmic leaflet of DIGs is strongly suggested on the basis of the known cell surface location of the majority of GPI-proteins. Caveolin is embedded in the cytoplasmic leaflet of hcDIGs by both a hook-like TM and triple palmitoylation at the carboxy-terminus, $pp59^{Lyn}$ by dual acylation at the amino-terminus. Upon dissociation from and relief of inhibition by caveolin-1 (see Section 4), $pp59^{Lyn}$ undergoes activation and autophosphorylation and finally phosphorylates IRS-1 at tyrosine residues, which initiates insulin-mimetic signalling downstream to metabolic effector systems (glucose transport, antilipolysis; Ref. [40], this study). The interaction of $pp59^{Lyn}$ with IRS-1/2 is facilitated by the "platform or bridging molecule", $pp125^{Fak}$, which also undergoes tyrosine (auto)phosphorylation [42].

constituted of rings ranging from a liquid-ordered cholesterol- and glycosphingolipid-enriched core through less ordered regions into the liquid-disordered non-DIG areas of the residual PM, the core of which is left as hcDIGs after TX-100 solubilization, whereas core and immediately surrounding areas are left unsolubilized by Lubrol-WX. Homogenous DIGs are liquid-ordered domains of a uniform mixture of the protein and lipid constituents are surrounded by the liquid-disordered phase of the PM which are selectively solubilized by TX-100 and Lubrol-WX [69]. Both models can hardly explain the existence of TX-100-insoluble lcDIGs or their generation from hcDIGs in response to glimepiride. In contrast, heterogenous DIGs of different lipid and protein composition could coexist as separate structural entities in the membrane and be differentially solubilized by TX-100 and Lubrol-WX. It is conceivable that the glimepiride-induced translocation of certain GPI-anchored and acylated signalling proteins from distinct hcDIGs accompanied by the limited loss of cholesterol results in the de novo generation of lcDIGs of increased buoyant density retaining TX-100 insolubility to a partial degree. Alternatively, the translocated DIG protein components may be recruited directly from discrete hcDIGs into pre-existing Lubrol-WX-insoluble (TX-100-soluble) lcDIGs thereby rendering them partially insoluble in TX-100.

In conclusion, regulation of the localization (redistribution within DIGs and dissociation from caveolin) and activation of the acylated signalling protein, $pp59^{Lyn}$, in rat adipocytes was elucidated using GPI-2350. This novel inhibitor of GPI-PLC may represent a useful biochemical tool for delineation of the diverse cellular functions of (G)PI-PLC/D in bacteria, protozoa and mammalian cells (see Section 1), in general. In particular, the adipocyte GPI-PLC has now been recognized as a critical component specifically operating in the insulin-mimetic signalling cascade triggered by glimepiride rather than in insulin signalling. Furthermore, insulin-mimetic signalling by glimepiride is not significantly impaired in the insulin-resistant state as reported previously for rat adipocytes in vitro [49]. Therefore, the adipocyte GPI-PLC might represent a useful target for the therapy of non-insulin-dependent diabetes mellitus. Its identification in near future should be facilitated by using a radiolabelled or biotinylated and photoactivatable derivate of GPI-2350.

References

[1] Nosjean O, Briolay A, Roux B. 1997 Mammalian GPI proteins: sorting, membrane residence and functions. Biochim Biophys Acta 1997;1331:153–86.

[2] Spychala J, Madrid-Marina V, Fox IH. Evidence for low K_m and high K_m soluble 5′-nucleotidase in human tissues and rat liver. Adv Exp Med Biol 1989;253B:129–34.

[3] Almqvist P, Carlsson SR. Characterization of a hydrophilic form of Thy-1 purified from human cerebrospinal fluid. J Biol Chem 1988; 263:12709–15.

[4] Sykes E, Ghag S, Epstein E, Kiechle FL. Effect of insulin, *S*-adenosylhomocysteine, phospholipase C, *n*-butanol and Triton X-114 on alkaline phosphatase from isolated rat adipocyte plasma membranes. Clin Chim Acta 1987;169:133–9.

[5] Huizinga TW, van der Schoot CE, Jost C, Klaassen R, Kleijer M, Roos D, et al. The PI-linked receptor FcRIII is released on stimulation of neutrophils. Nature 1988;333:667–9.

[6] Suh PG, Ryu SH, Moon KH, Suh HW, Rhee SG. Inositol phospholipid-specific phospholipase C: complete cDNA and protein sequences and sequence homology to tyrosine kinase-related oncogene products. Proc Natl Acad Sci USA 1988;85:5419–23.

[7] Eliakim R, Becich MJ, Green K, Alpers DH. Both tissue and serum phospholipases release rat intestinal alkaline phosphatase. Am J Physiol 1990;259:G618–25.

[8] Roberts JM, Kenon P, Johnson PM. Growth factor-induced release of a glycosyl-phosphatidylinositol (GPI)-linked protein from the HEP-2 human carcinoma cell line. FEBS Lett 1990;267:213–6.

[9] Englund PT. The structure and biosynthesis of glycosylphosphatidylinositol protein anchors. Annu Rev Biochem 1993;62:121–38.

[10] Park SW, Choi K, Kim IC, Lee HH, Hooper NM, Park HS. Endogenous glycosylphosphatidylinositol-specific phospholipase C releases renal dipeptidase from kidney proximal tubules in vitro. Biochem J 2001;353:339–44.

[11] Fox JA, Soliz NM, Saltiel AR. Purification of a phosphatidylinositol-glycan specific phospholipase C from liver plasma membranes: a possible target of insulin action. Proc Natl Acad Sci USA 1987; 84:2663–7.

[12] Hari T, Butikofer P, Wiesmann UN, Brodbeck U. Uptake and intracellular stability of glycosylphosphatidylinositol-specific phospholipase D in neuroblastoma cells. Biochim Biophys Acta 1997;1355: 293–302.

[13] Low MG, Huang KS. Factors affecting the ability of glycosylphosphatidylinositol-specific phospholipase D to degrade the membrane anchors of cell surface proteins. Biochem J 1991;279:483–93.

[14] Müller G, Dearey E-A, Körndörfer A, Bandlow W. Stimulation of a glycosyl phosphatidylinositol-specific phospholipase by insulin and the sulfonylurea, glimepiride, in rat adipocytes depends on increased glucose transport. J Cell Biol 1994;126:1267–76.

[15] Müller G, Groβ E, Wied S, Bandlow W. Glucose-induced sequential processing of a glycosyl-phosphatidylinositol-anchored ectoprotein in *Saccharomyces cerevisiae*. Mol Cell Biol 1996;16:442–56.

[16] Müller G, Bandlow W. Glucose induces lipolytic cleavage of a glycolipidic plasma membrane anchor in yeast. J Cell Biol 1993;122:325–36.

[17] Müller G, Wetekam E-M, Jung C, Bandlow W. Membrane association of lipoprotein lipase and a cAMP-binding ectoprotein in rat adipocytes. Biochemistry 1994;33:12149–59.

[18] Müller G, Bandlow W. Lipolytic membrane release of two phosphatidylinositol-anchored cAMP receptor proteins in yeast alters their ligand-binding parameters. Arch Biochem Biophys 1994;308:504–14.

[19] Barton PL, Futerman AH, Silman I. Arrhenius plots of acetylcholine esterase activity in mammalian erythrocytes and in Torpedo electric organ. Effect of solubilization by proteinases and by phosphatidylinositol-specific phospholipase C. Biochem J 1985;231:237–40.

[20] Klip A, Ramlal T, Douen AG, Burdett E, Young D, Cartee GD, et al. Insulin-induced decrease in 5-nucleotidase activity in skeletal muscle membranes. FEBS Lett 1988;238:419–23.

[21] Braun-Breton C, Rosenberry TL, Da Silva LP. Induction of the proteolytic activity of a membrane protein in *Plasmodium falciparum* by phosphatidylinositol-specific phospholipase C. Nature 1988;332: 457–9.

[22] Brewis IA, Turner AJ, Hooper NM. Activation of the glycosylphosphatidylinositol-anchored membrane dipeptidase upon release

from pig kidney membranes by phospholipase C. Biochem J 1994; 303:633–8.
[23] Schroeder R, London E, Brown DA. Interactions between saturated acyl chains confer detergent resistance on lipids and glycosylphosphatidylinositol (GPI)-anchored proteins: GPI-anchored proteins in liposomes and cells show similar behavior. Proc Natl Acad Sci USA 1994;91:12130–4.
[24] Sharom FY, Lehto MT. Glycosylphosphatidylinositol-anchored proteins: structure, function, and cleavage by phosphatidylinositol-specific phospholipase C. Biochem Cell Biol 2002;80:535–49.
[25] Bandlow W, Wied S, Müller G. Glucose induces amphiphilic to hydrophilic conversion of a subset of glycosyl-phosphatidylinositol-anchored ectoproteins in yeast. Arch Biochem Biophys 1995; 324:300–16.
[26] Lu C-F, Kurjan J, Lipke PN. A pathway for cell wall anchorage of *Saccharomyces cerevisiae* α-agglutinin. Mol Cell Biol 1994;14: 4825–33.
[27] Accardo-Palumbo AG, Triolo G, Colonna-Romano M, Potestio M, Carbone A, Ferrante E, et al. Glucose-induced loss of glycosyl-phosphatidylinositol-anchored membrane regulators of complement activation (CD59, CD55) by in vitro cultured human umbilical vein endothelial cells. Diabetologia 2000;43:1039–47.
[28] Chan BL, Lisanti MP, Rodriguez-Boulan E, Saltiel AR. Insulin-stimulated release of lipoprotein lipase by metabolism of its phosphatidylinositol anchor. Science 1988;241:1670–2.
[29] Lisanti MP, Darnell JC, Chan BL, Rodriguez-Boulan E, Saltiel AR. The distribution of glycosyl-phosphatidylinositol anchored proteins is differentially regulated by serum and insulin. Biochim Biophys Res Commun 1989;164:824–32.
[30] Movahedi S, Hooper NM. Insulin stimulates the release of the glycosyl phosphatidylinositol-anchored membrane dipeptidase from 3T3-L1 adipocytes through the action of a phospholipase C. Biochem J 1997;326:531–7.
[31] Spooner PM, Chernick SS, Garrison MM, Scow RO. Insulin regulation of lipoprotein lipase activity and release in 3T3-L1 adipocytes. J Biol Chem 1979;254:10021–9.
[32] Müller G. The molecular mechanism of the insulin-mimetic/sensitizing activity of the antidiabetic sulfonylurea drug amaryl. Mol Med 2000;6:907–33.
[33] Müller G, Geisen K. Characterization of the molecular mode of the sulphonylurea, glimepiride, at adipocytes. Horm Metab Res 1996; 28:469–87.
[34] Müller G. Dynamics of plasma membrane microdomains and cross-talk to the insulin signalling cascade. FEBS Lett 2002;531: 81–7.
[35] Brown DA, London E. Structure and function of sphingolipid- and cholesterol-rich membrane rafts. J Biol Chem 2000;275:17221–4.
[36] Friedrichson T, Kurzchalia TV. Microdomains of GPI-anchored proteins in living cells revealed by crosslinking. Nature 1998;394: 802–5.
[37] Smart EJ, Graf GA, McNiven MA, Sessa WC, Engelman JA, Scherer PE, et al. Caveolins, liquid-ordered domains, and signal transduction. Mol Cell Biol 1999;19:7289–304.
[38] Müller G, Hanekop N, Wied S, Frick W. Cholesterol depletion blocks redistribution of lipid raft components and insulin-mimetic signalling by glimepiride and phosphoinositolglycans in rat adipocytes. Mol Med 2002;8:120–36.
[39] Frick W, Bauer A, Bauer J, Wied S, Müller G. Structure-activity relationship of synthetic phosphoinositolglycans mimicking metabolic insulin action. Biochemistry 1998;37:13421–36.
[40] Müller G, Jung C, Wied S, Welte S, Jordan H, Frick W. Redistribution of glycolipid raft domain components induces insulin-mimetic signalling in rat adipocytes. Mol Cell Biol 2001;21:4553–67.
[41] Müller G, Wied S, Piossek C, Bauer A, Bauer J, Frick W. Convergence and divergence of the signalling pathways for insulin and phosphoinositolglycans. Mol Med 1998;4:299–323.
[42] Müller G, Wied S, Frick W. Cross talk of $pp125^{Fak}$ and $pp59^{Lyn}$ non-receptor tyrosine kinases to insulin-mimetic signalling in adipocytes. Mol Cell Biol 2000;20:4708–23.
[43] Müller G, Jordan H, Petry S, Wetekam E-M, Schindler P. Analysis of lipid metabolism in adipocytes using a fluorescent fatty acid derivative. I. Insulin stimulation of lipogenesis. Biochem Biophys Acta 1997;1347:23–39.
[44] Zhai H-X, Ping-Shen L, Morris JC, Mensa-Wilmot K, Shen TY. Synthesis of 2-deoxy-2-fluorinated inositol-1-*O*-dodecylphosphonates as inhibitors of glycosyl phosphatidylinositol phospholipase C. Tetrahydron Lett 1995;36:7403–6.
[45] Mensa-Wilmot K, Morris JC, Al-Qahtani A, Englund PT. Purification and use of recombinant glycosylphosphatidylinositol-phospholipase C. Meth Enzymol 1995;250:641–55.
[46] Stieger S, Brodbeck U. Assay and purification of PI-specific phospholipase C from *Bacillus cereus* using commercially available phospholipase C. In: Brodbeck U, Bordier C, editors. Post-translational Modification of Proteins by Lipids — A Laboratory Manual. Berlin: Springer; 1988. p. 34–9.
[47] Vertesy L, Beck B, Brönstrup M, Ehrlich K, Kurz M, Müller G, et al. Cyclipostins, novel hormone-sensitive lipase inhibitors from *Streptomyces* sp. DSM 13381. II. Isolation, structure elucidation and biological properties. J Antibiotics 2002;55:480–94.
[48] Kim T-S, Sundaresh CS, Feinstein SJ, Dodia C, Skach WR, Jain MK, et al. Identification of a human cDNA clone for lysosomal type Ca^{2+}-independent phospholipase A_2 and properties of the expressed protein. J Biol Chem 1997;272:2542–50.
[49] Müller G, Wied S. The sulfonylurea drug, glimepiride, stimulates glucose transport, glucose transporter translocation, and dephosphorylation in insulin-resistant rat adipocytes in vitro. Diabetes 1993; 42:1852–67.
[50] Bordier C. Phase separation of integral membrane proteins in Triton X-114 solution. J Biol Chem 1981;256:1604–7.
[51] Müller G, Jordan H, Jung C, Kleine H, Petry S. Analysis of lipolysis in adipocytes using a fluorescent fatty acid derivative. Biochimie 2003;85:1245–56.
[52] Müller G, Wied S, Wetekam E-M, Crecelius A, Unkelbach A, Pünter J. Stimulation of glucose utilization in 3T3 adipocytes and rat diaphragm *in vitro* by the sulphonylureas, glimepiride and glibenclamide, is correlated with modulations of the cAMP regulatory cascade. Biochem Pharmacol 1994;48:985–96.
[53] Müller G, Dearey E-A, Pünter J. The sulphonylurea drug, glimepiride, stimulates release of glycosyl-phosphatidylinositol-anchored plasma membrane proteins from 3T3 adipocytes. Biochem J 1993;289: 509–21.
[54] Lehto MT, Sharom FJ. Release of the glycosylphosphatidylinositol-anchored enzyme ecto-5-nucleotidase by phospholipase C: catalytic activation and modulation by the lipid bilayer. Biochem J 1998; 332:101–9.
[55] Lewis KA, Garigapati VR, Zhou C, Roberts MF. Substrate requirements of bacterial phosphatidylinositol-specific phospholipase C. Biochemistry 1993;32:8836–41.
[56] Roberts JM, Myher JJ, Kuksis A, Low MG, Rosenberry TL. Lipid analysis of the glycoinositol phospholipid membrane anchor of human erythrocyte acetylcholine esterase. Palmitoylation of inositol results in resistance to phosphatidylinositol-specific phospholipase C. J Biol Chem 1988;263:18766–75.
[57] Morris JC, Ping-Shen L, Zhai H-X, Shen T-Y, Mensa-Wilmot K. Inhibition of GPI phospholipase C from *Trypanosoma brucei* by fluoro-inositol dodecylphosphonates. Biochem Biophys Res Commun 1998;244:873–6.
[58] Dodson G, Wlodawer A. Catalytic triads and their relatives. Trends Biochem Sci 1998;23:347–52.
[59] Morris JC, Ping-Sheng L, Zhai HX, Shen T-Y, Mensa-Wilmot K. Phosphatidylinositol phospholipase C is activated allosterically by the aminoglycoside G418. J Biol Chem 1996;271:15468–77.

[60] Morris JC, Ping-Sheng L, Shen T-Y, Mensa-Wilmot K. Glycan requirements of glycosylphosphatidylinositol phospholipase C from *Trypanosoma brucei*. J Biol Chem 1995;270:2517–24.
[61] Müller G, Hanekop N, Kramer W, Bandlow W, Frick W. Interaction of phosphoinositolglycan(peptides) with plasma membrane lipid rafts of rat adipocytes. Arch Biochem Biophys 2002;408:17–32.
[62] Röper K, Corbeil D, Huttner WB. Retention of prominin in microvilli reveals distinct cholesterol-based lipid microdomains in the apical plasma membrane. Nat Cell Biol 2002;2:582–92.
[63] Müller G, Jung C, Frick W, Bandlow W, Kramer W. Interaction of phosphatidylinositolglycan(peptides) with plasma membrane lipid rafts triggers insulin-mimetic signalling in rat adipocytes. Arch Biochem Biophys 2002;408:7–16.
[64] Couet J, Li S, Okamoto T, Ikezu T, Lisanti MP. Identification of peptide and protein ligands for the caveolin-scaffolding domain. J Biol Chem 1997;272:6525–33.
[65] Li S, Couet J, Lisanti MP. Src tyrosine kinases, Galpha subunits, and H-Ras share a common membrane-anchored scaffolding protein, caveolin. Caveolin binding negatively regulates the auto-activation of Src tyrosine kinases. J Biol Chem 1996;272:29182–90.
[66] Müller G, Frick W. Signalling via caveolin: involvement in the cross-talk between phosphoinositolglycans and insulin. Cell Mol Life Sci 1999;56:945–70.
[67] Okamoto T, Schlegel A, Scherer PE, Lisanti MP. Caveolins, a family of scaffolding proteins for organizing ''preassembled signalling complexes'' at the plasma membrane. J Biol Chem 1998;273:5419–22.
[68] Sekar N, Li J, Schechter Y. Vanadium salts as insulin substitutes: mechanisms of action, a scientific and therapeutic tool in diabetes mellitus research. Crit Rev Biochem Mol Biol 1996;31:339–59.
[69] Pike LJ. Lipid rafts: heterogeneity on the high seas. Biochem J 2004;378:281–92.